

Thermal-hydraulics of Nuclear Reactors

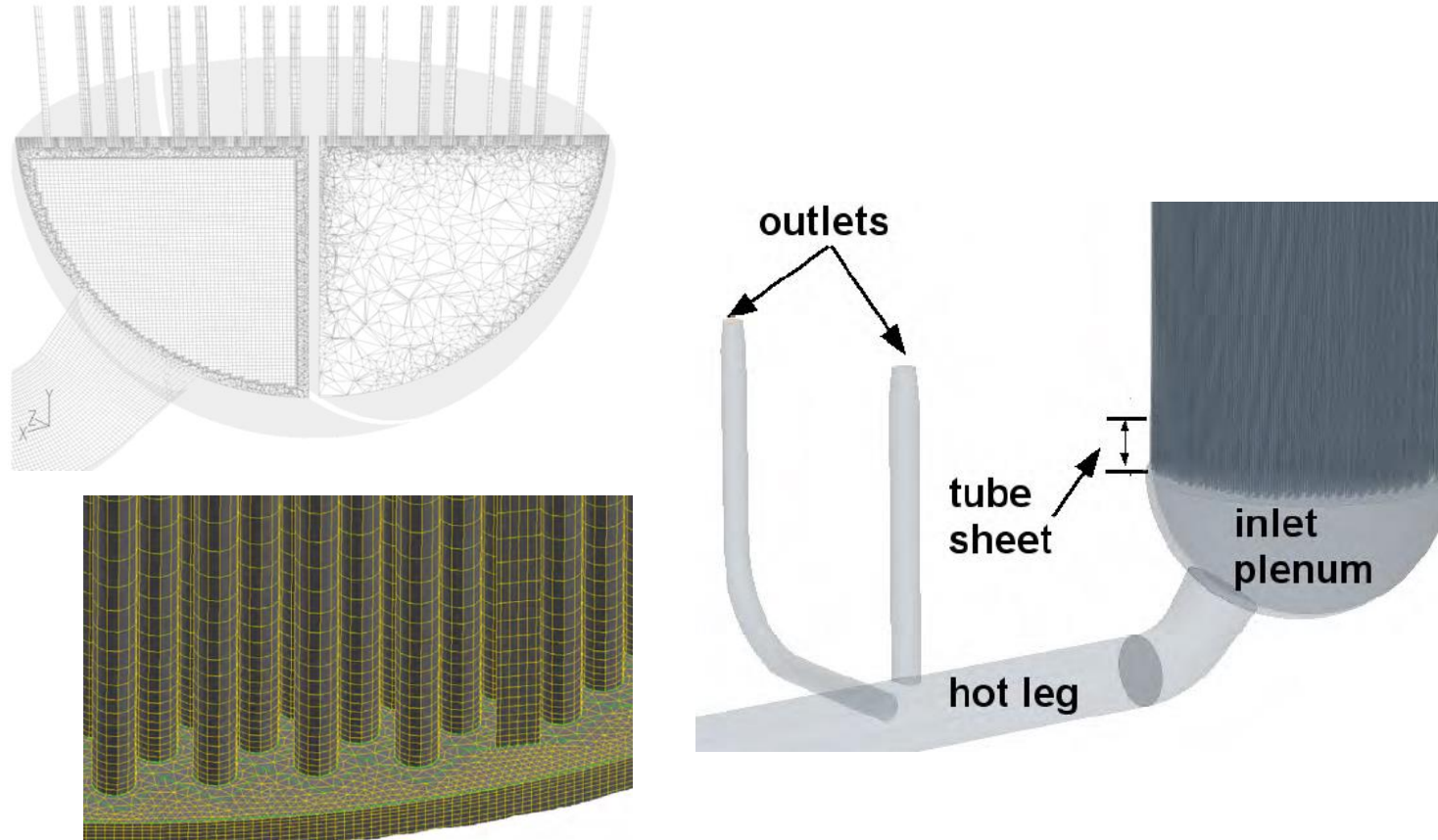
ADVANCED MODELLING & SIMULATION – AMS –

WWW.AFRY.COM/AMS

DJAMEL.LAKEHAL@AFRY.COM

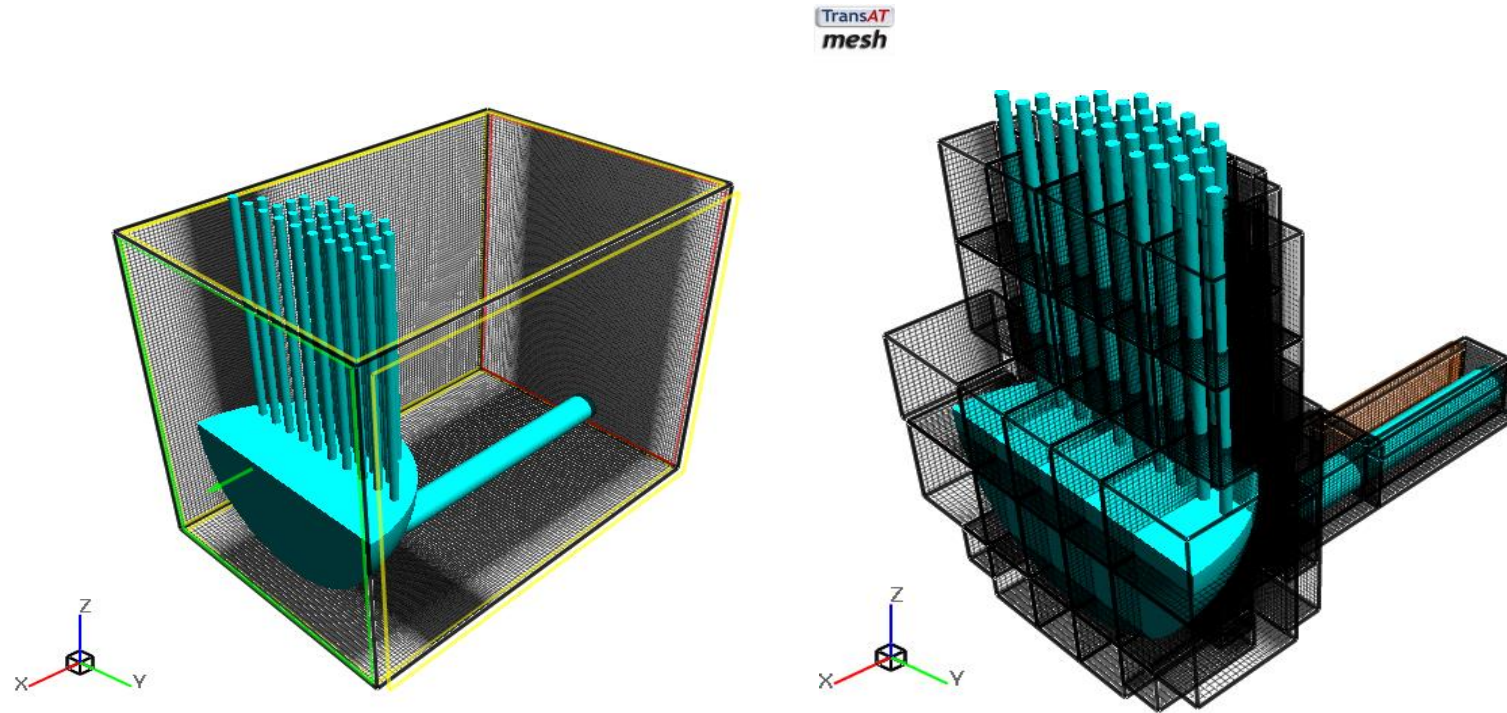
JULY 2018

Flow in Steam Generators: Fluent grid



- **Courtesy: NRC (Chris Boyd, FLUENT)**

Flow in Steam Generators: TransAT grid



- **ASCOMP (TransAT)**

Fluent & TransAT solutions

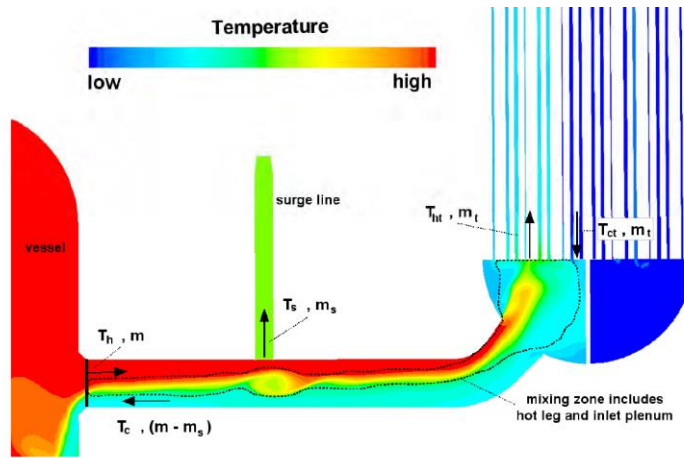
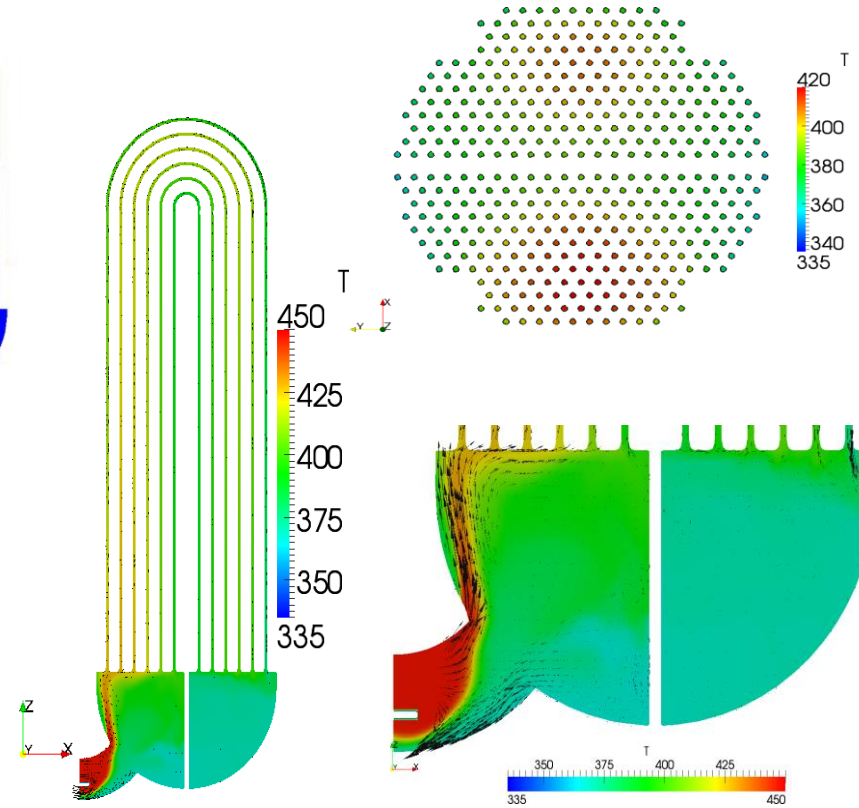


Figure 13. CFD Predictions Indicating Expanded Mixing Region

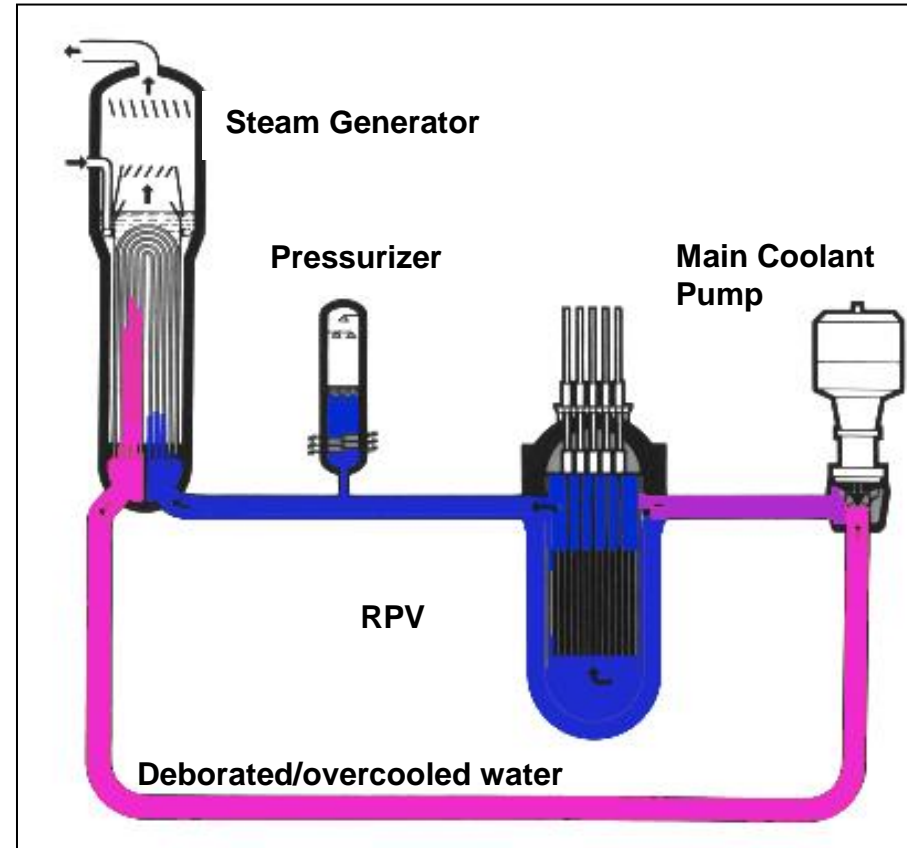
- **NRC (Fluent)**



- **ASCOMP (TransAT)**

Boron mixing in PWR primary circuit

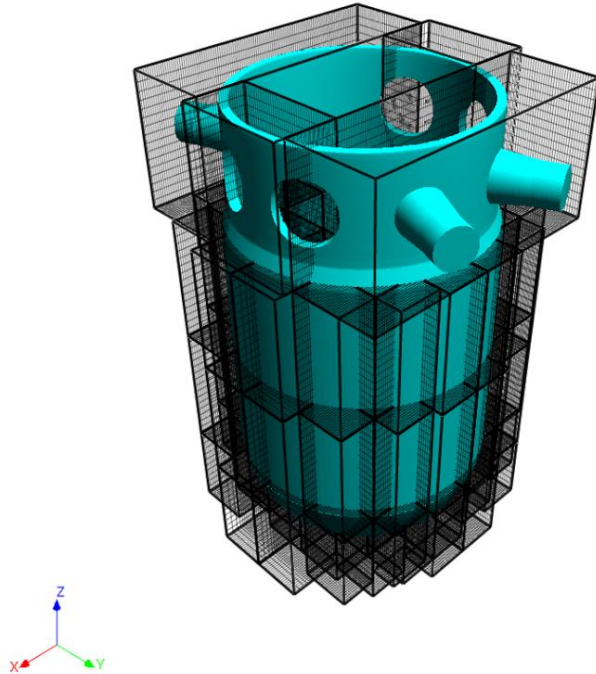
- PWR is equipped with 2 or more loops (German KONVOI: 4)
- Boron dissolved in the coolant acts as neutron absorber
- Hypothetical accidents with creation of lower borated slugs in single loops
- Importance of mixing of coolant with different boron content



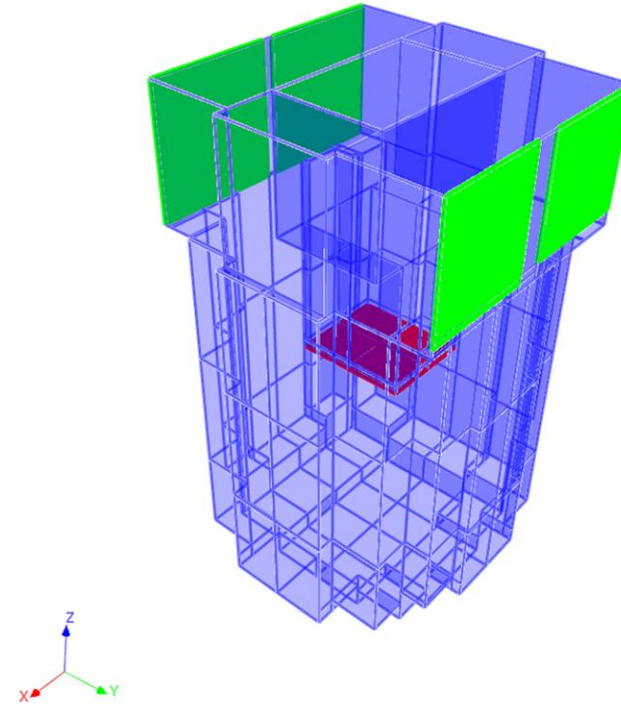
— Primary circuit of a PWR

ROCOM tests (SIEMENS Germany)

Boron dilution: 1D-3D Coupling (Cathare-transat)

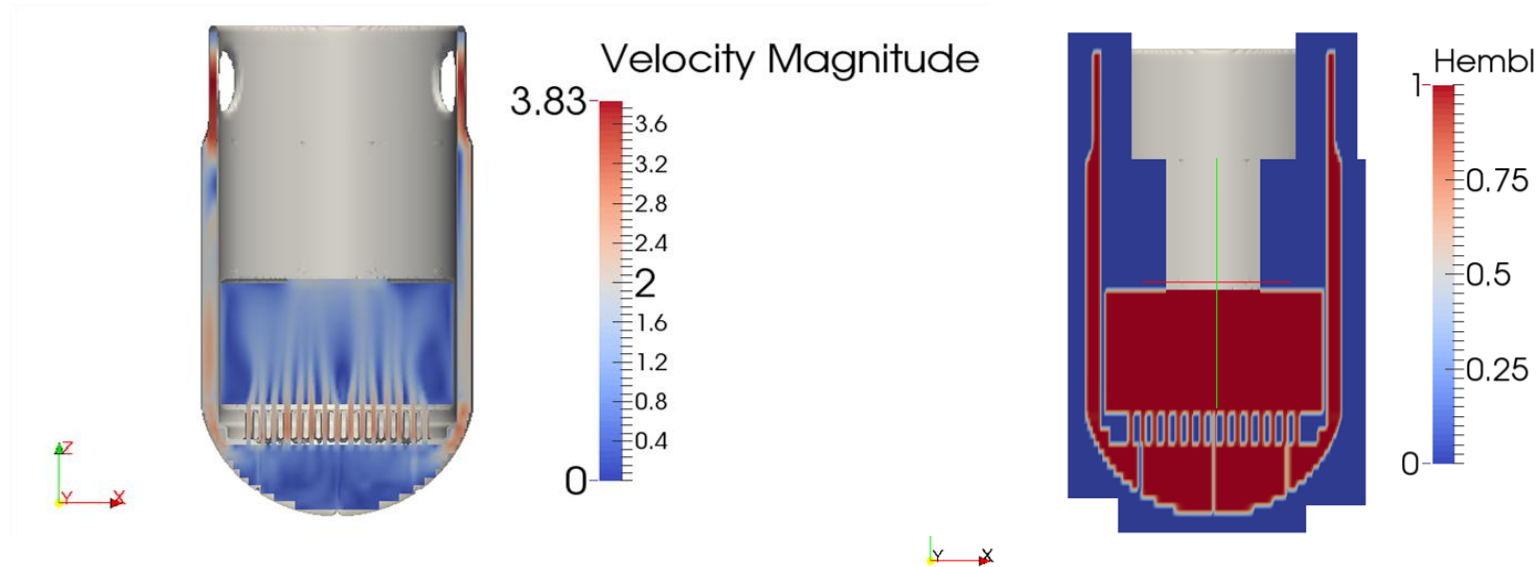


- The flow is simulated with TransAT.
- The fluid domain is shown in blue - everything else is solid (“inverted” view).
- IST mesh is created by using multiple blocks with a total of **700k** cells.



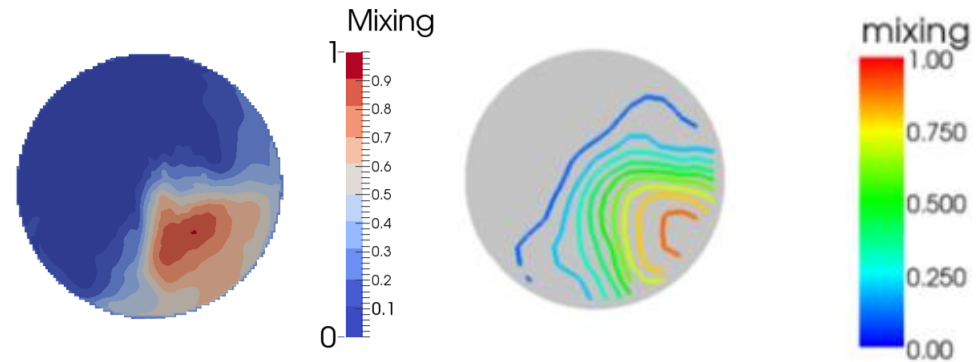
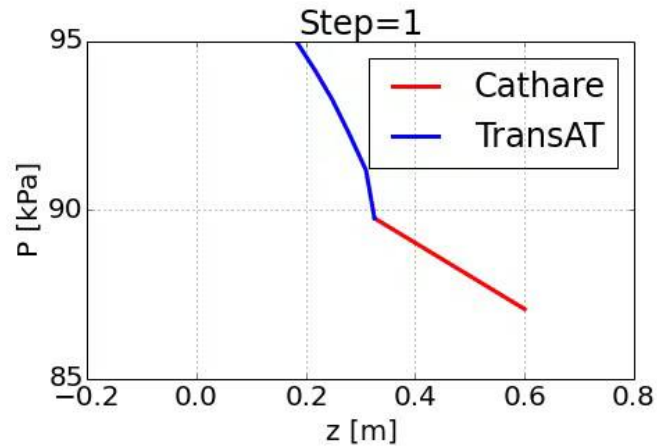
- The inlet boundaries, indicated by green surfaces, have velocity = 2.91m/s
- The outlet/coupling boundary is indicated by a red surface, with no prescribed conditions.

Boron dilution: 1D-3D Coupling (cathare-transat)



- Planes are perpendicular to the Y direction
- Fluid goes deep into the lower plenum, and then rises up through the support plate.
- Sharp interface is implemented, which creates gaps between adjacent objects. The unexpected gaps in the lower plenum will affect the fluid field.

Boron dilution: 1D-3D Coupling (cathare-transat)



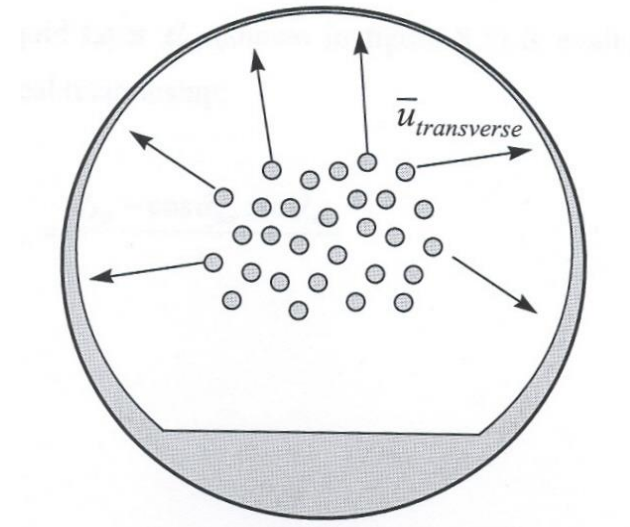
- With a larger time step, there are no significant pressure oscillations in CATHARE.
- At the coupling interface, pressure values from both sides match well.
- The maximum mixing scalar is very well captured by the coupled solution.
- The concentration spreading is only slightly underestimated compared to the data.

Droplet entrainment: The practical context

Air-water flow

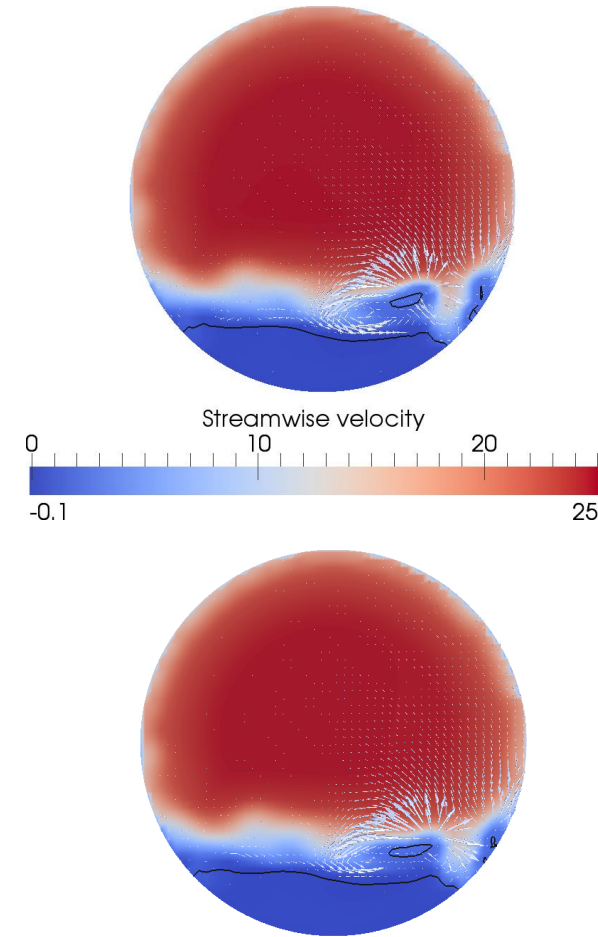
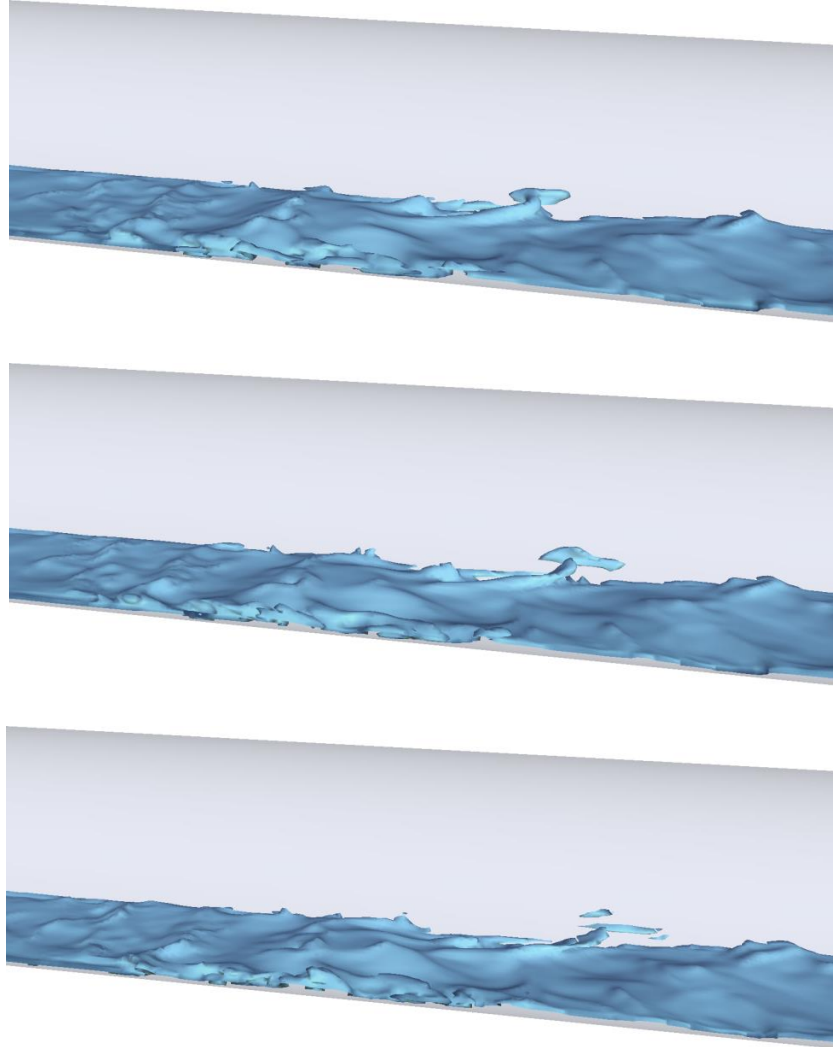


Wetting mechanism

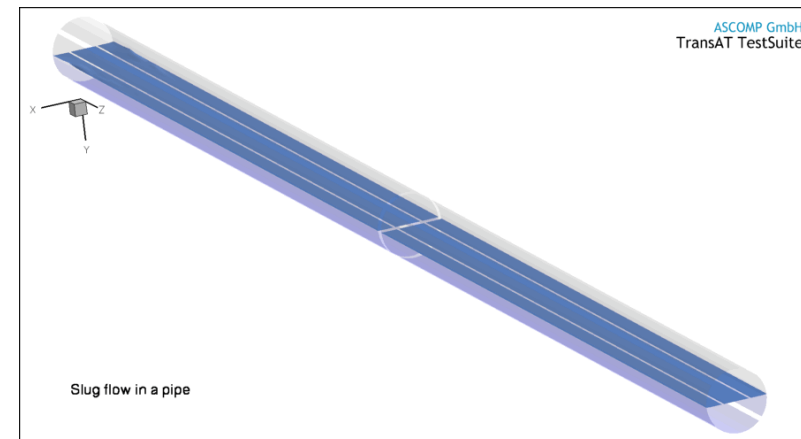
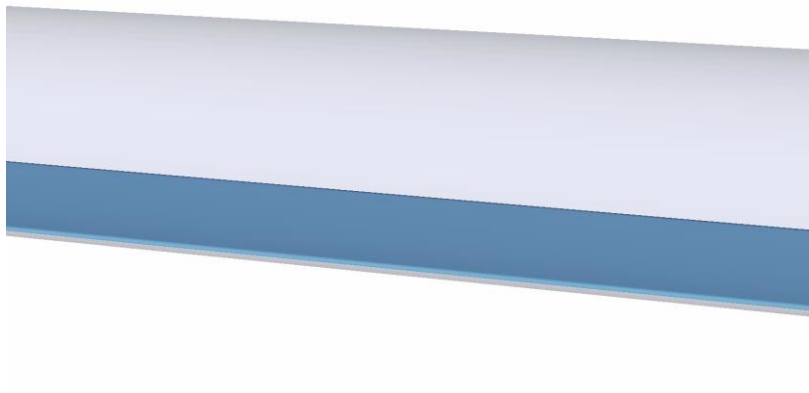
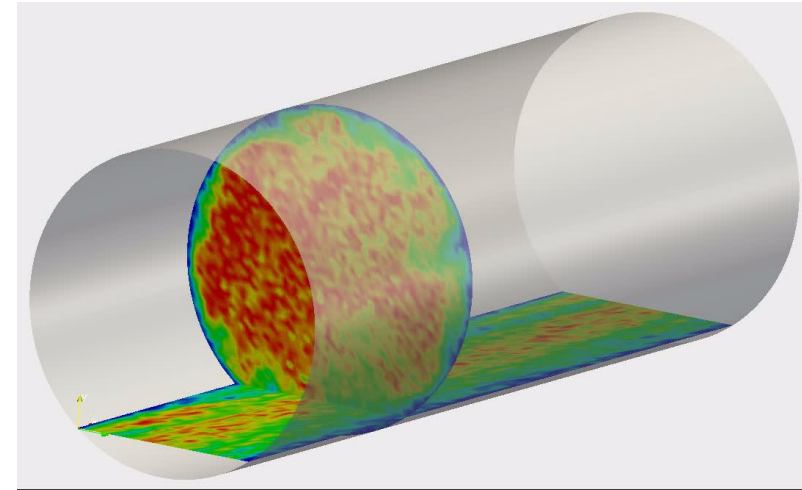
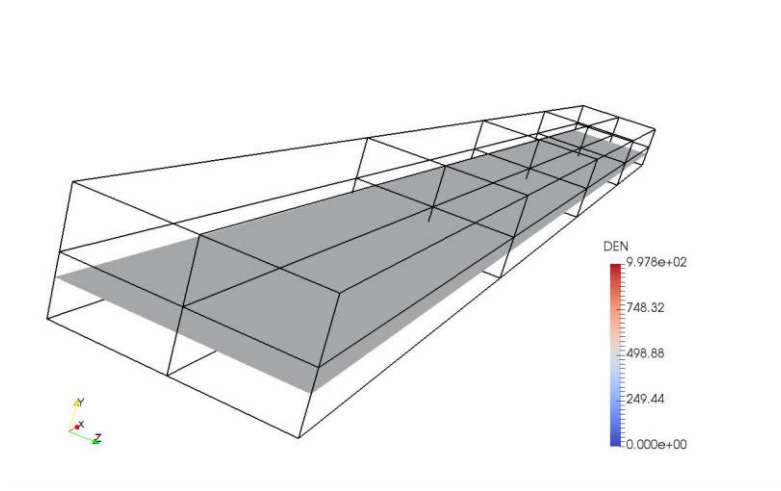


Courtesy: Badie & Hewitt © Imperial College London

LEIS of droplet entrainment in a pipe



Free-surface horizontal flows

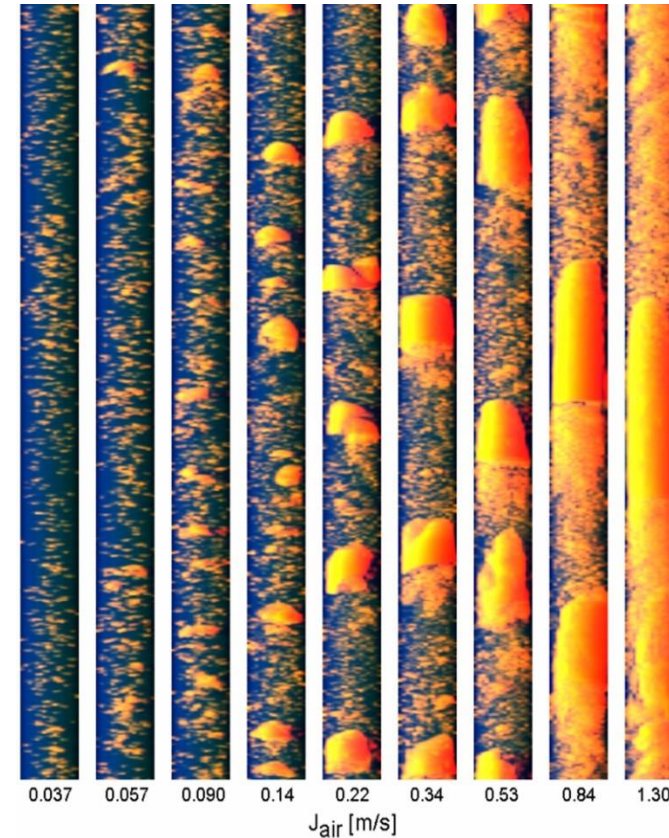


Vertical Flow: The Issues

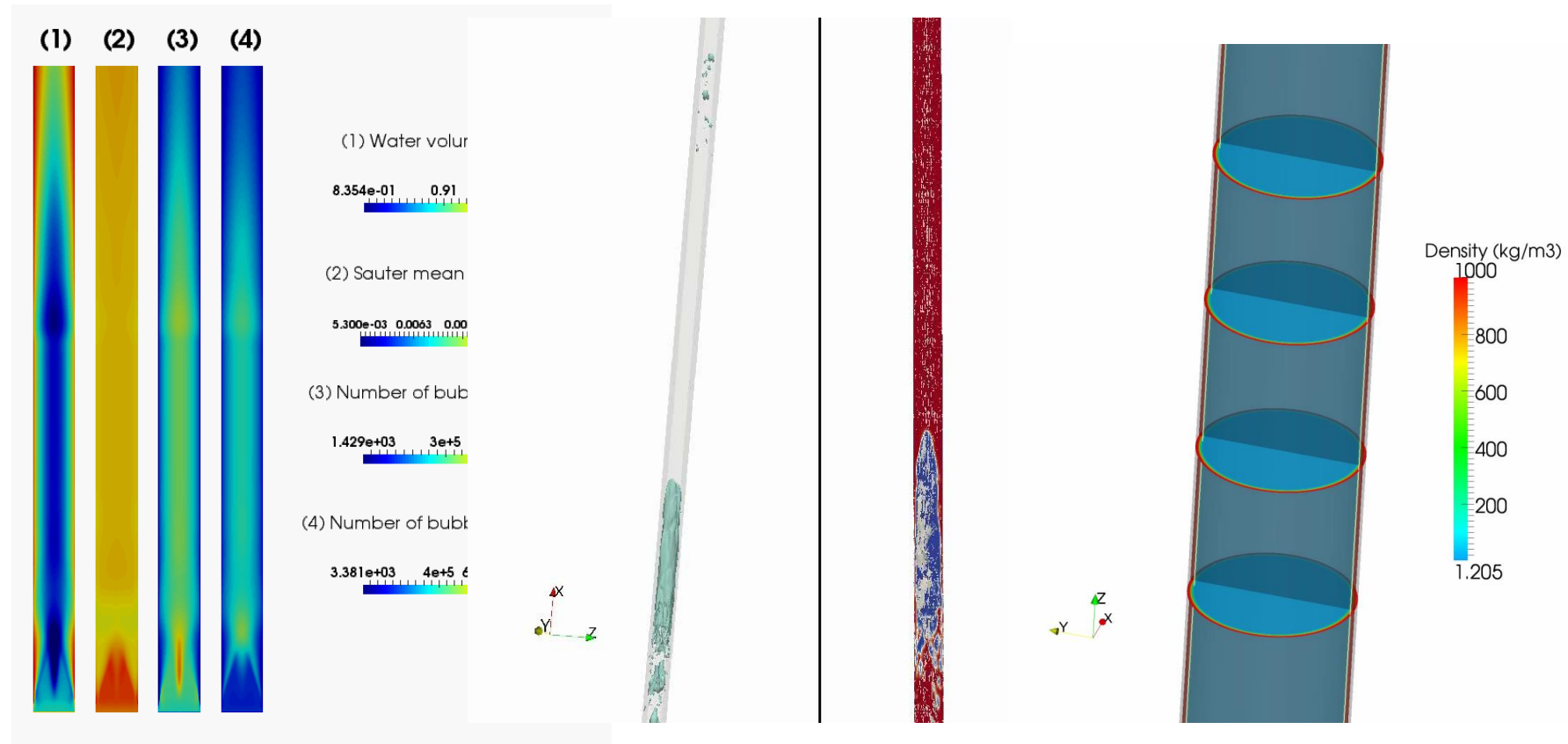
- Flow regime map definition (e.g. slug speeds & size, etc.)
- Phase distribution
- Pressure drop and thermal transients
- Large diameter risers.

Why CMFD?

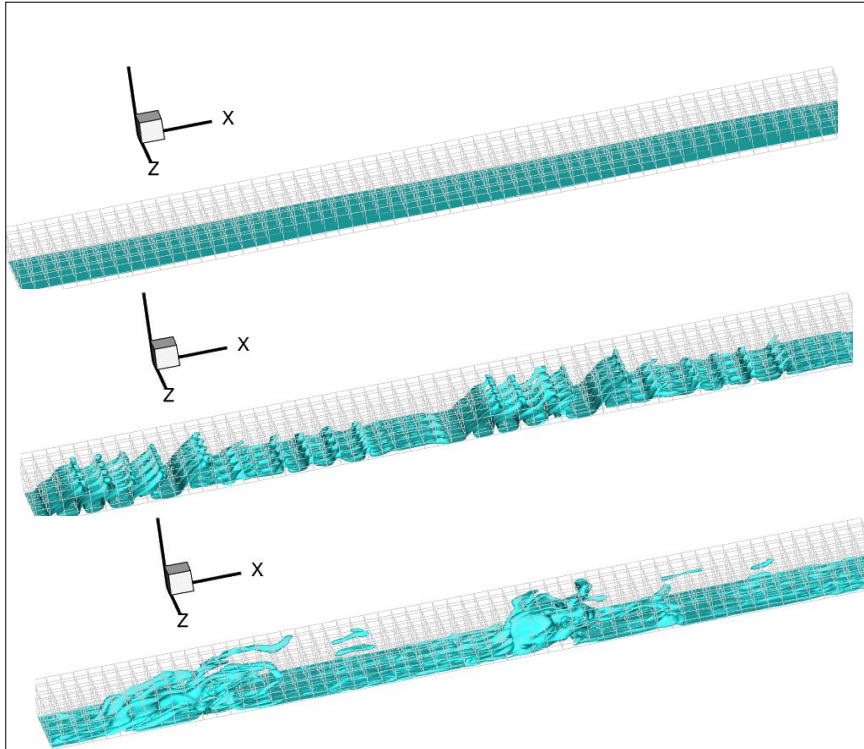
- Can simulate various flow regimes.
- Advanced models (ITM) are needed for certain flow patterns (e.g. slugging), and
- Can help identify flow regimes for large-diameter risers, as
- Shown in examples of next slide.



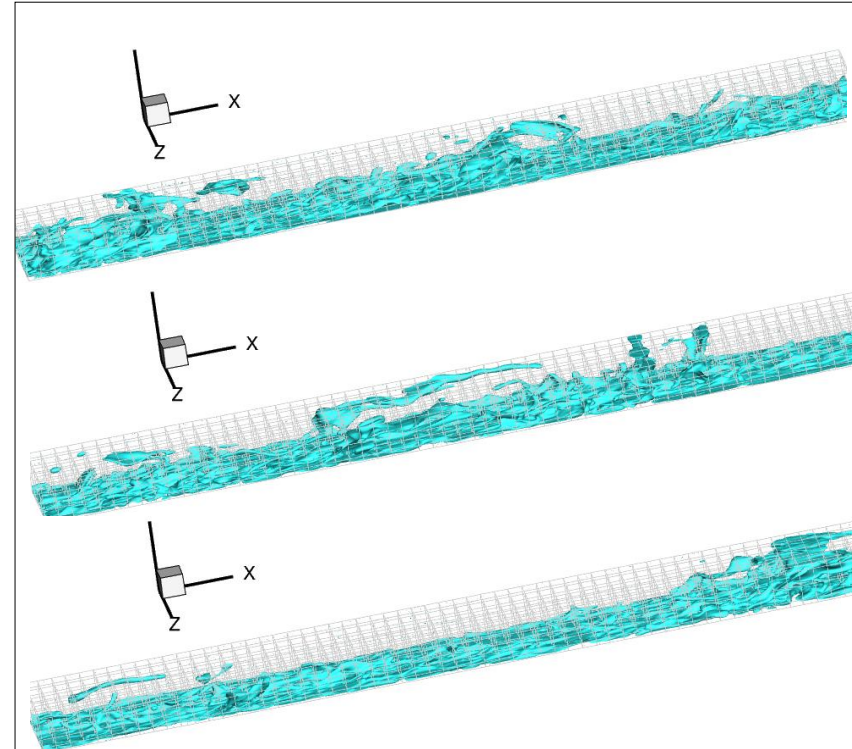
Flow Regime Prediction



Annular Flow (full domain)



- $J_g = 20$ m/s, $J_l = 1.5$ m/s. Comp. domain spans one full wavelength
- LEIS: Total number of grid points is 10 million cells distributed over 960 cores.



- Ligament formation, droplet detachment, formation of large disturbance wave clearly visible in these simulations
- Flow for full domain still developing.

Condensation of steam jets from a sparger in a pool (KEPCO Korea)

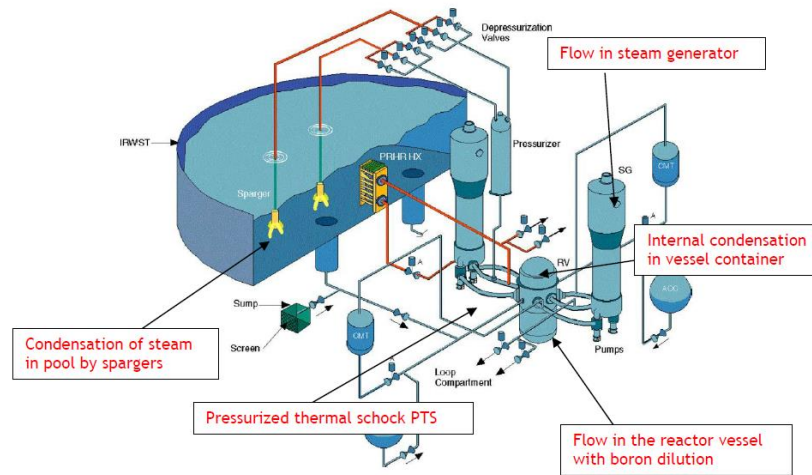
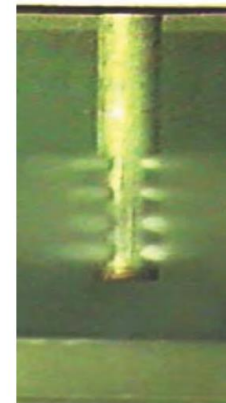
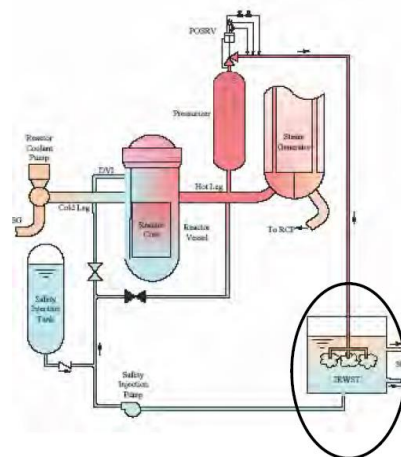
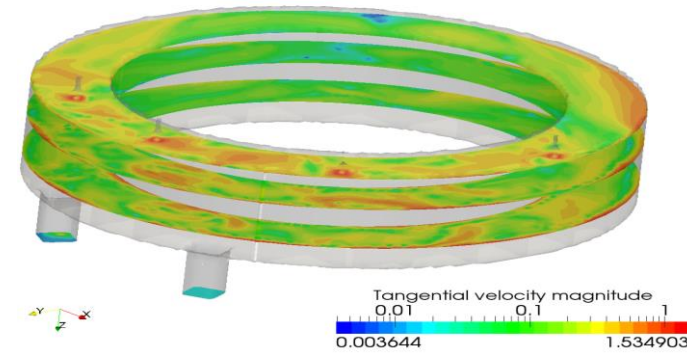


Figure 1: AP1000 RCS and passive core cooling system (Schulz, 2006)



Condensation of steam jets from a sparger in a pool (KEPCO Korea)

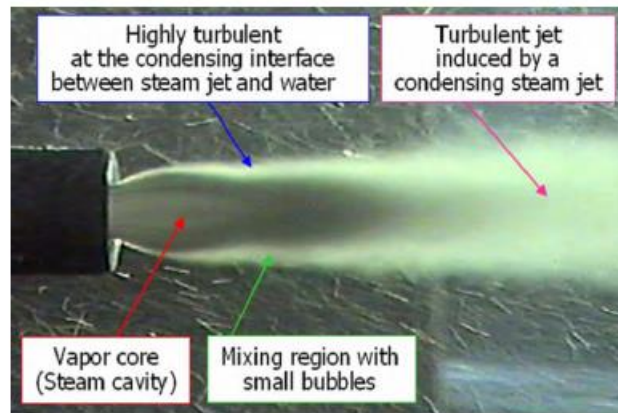
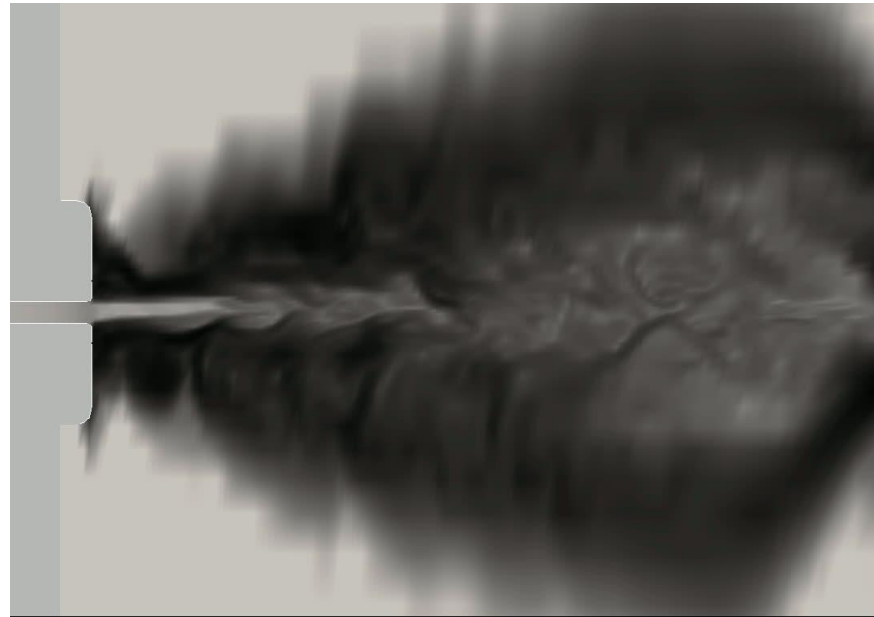
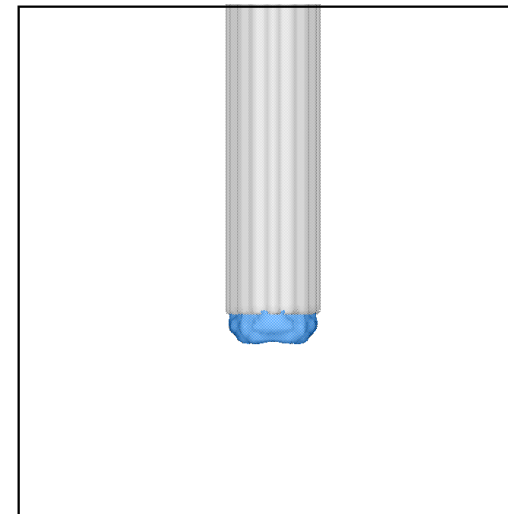
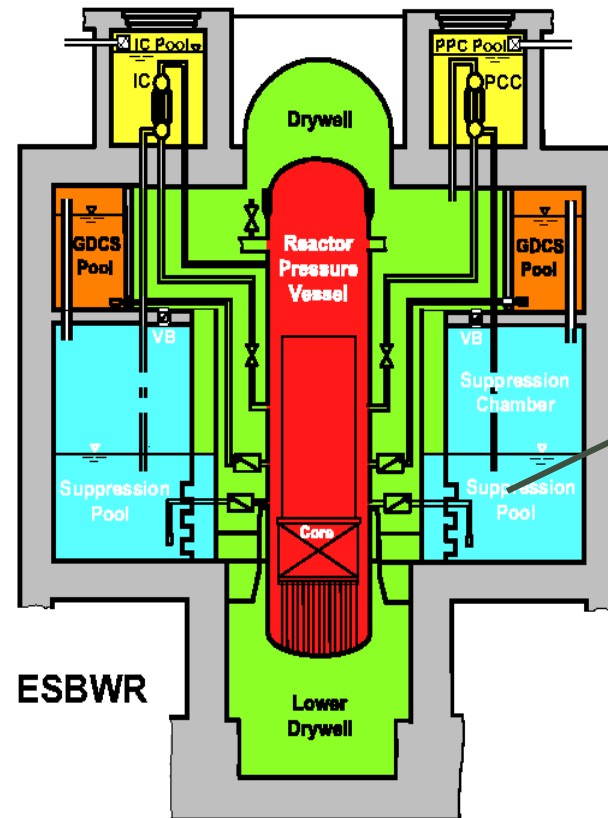


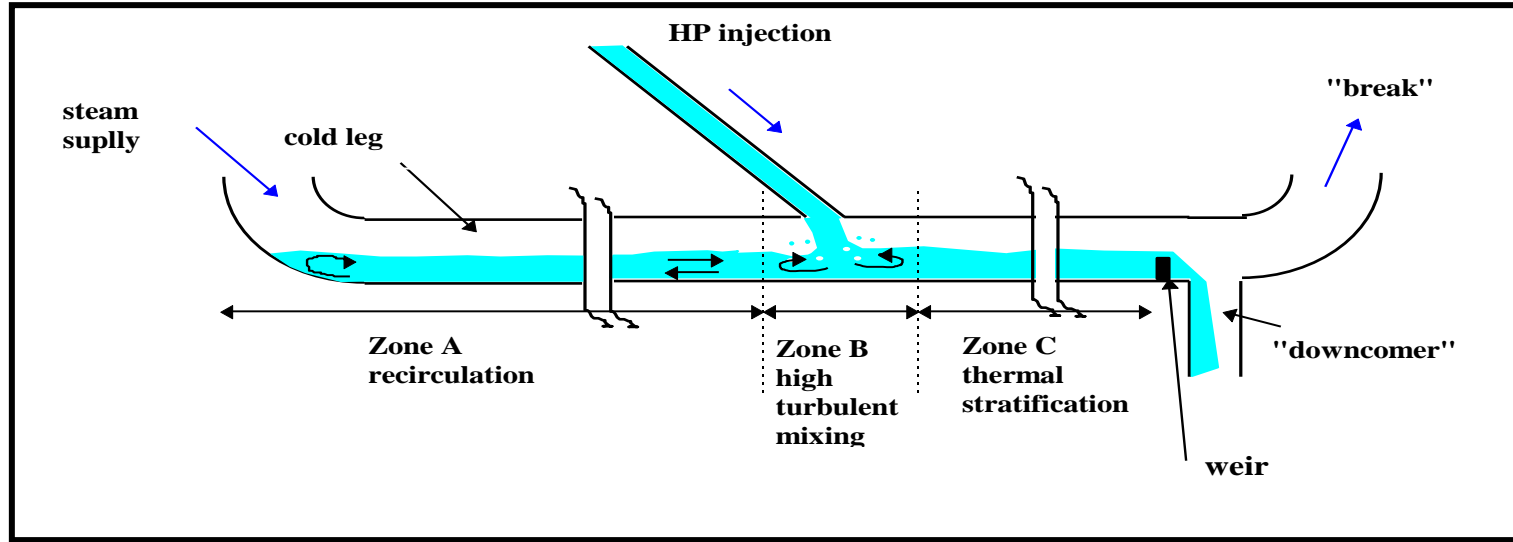
Image of condensing jet
from Song et al. (2012)



RPV de-pressurisation



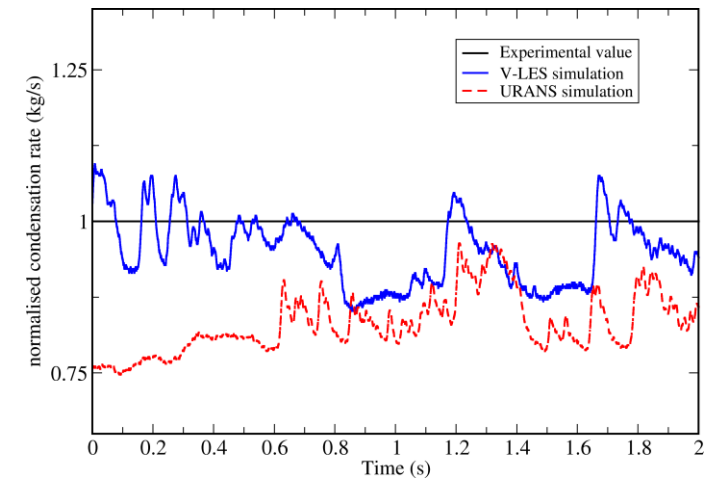
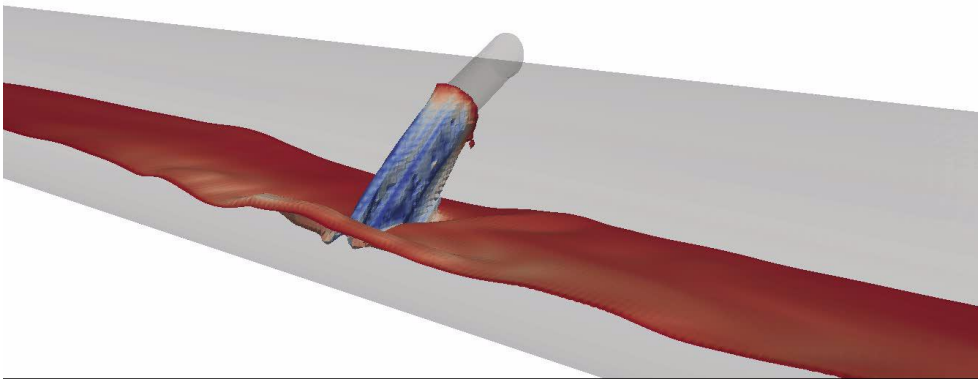
PTS: COSI Exp. (AREVA)



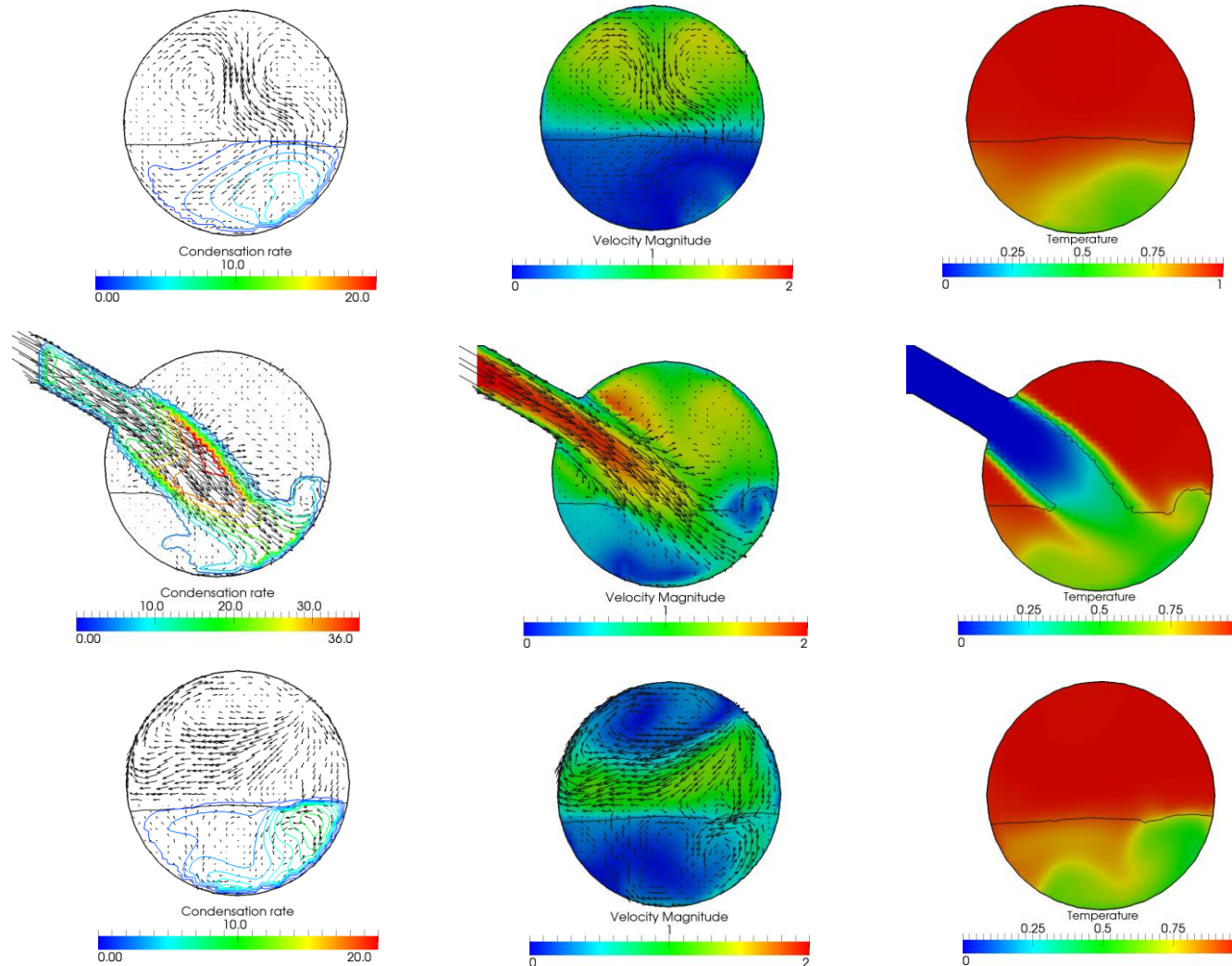
- **Courtesy from Yadigaroglu and Bestion, ICAPP07**
- During a hypothetical SB-LOCA, cold water is injected into the cold leg to limit the RPV lifetime (Emergency Core Cooling, ECC).
- The injected water mixes with the hot fluid in the cold leg and flows towards the downcomer leading to excessive thermal stresses on the RPV walls.

Rate of condensation

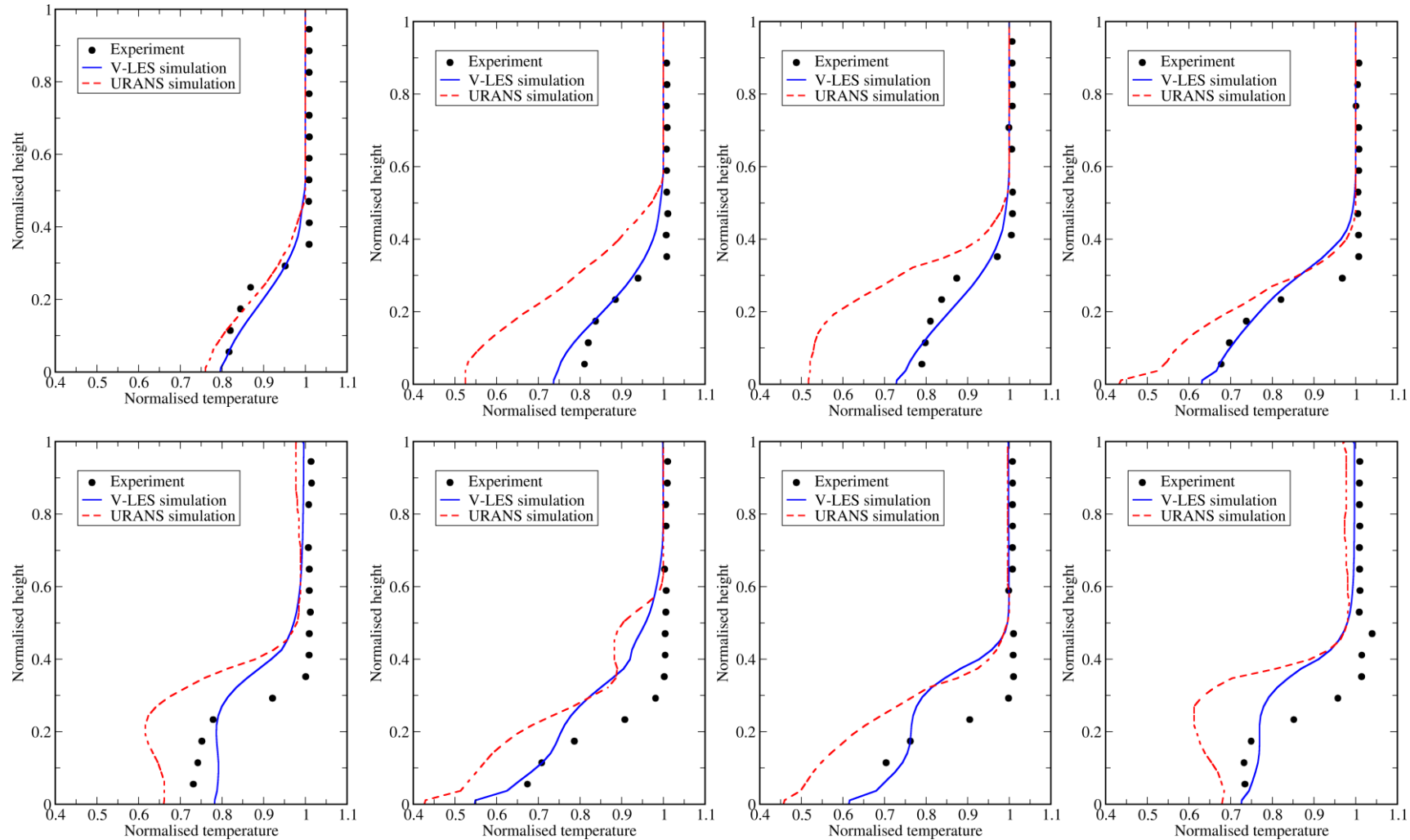
- ECC injection of cold water (296 K) in saturated water
- Steam at saturation temperature (485 K)
- Pressure 20 bars
- Simulation with TransAT level-set technique
- RANS vs. V-LES models for turbulence
- Interfacial condensation model (Labois & Lakehal, 2010)



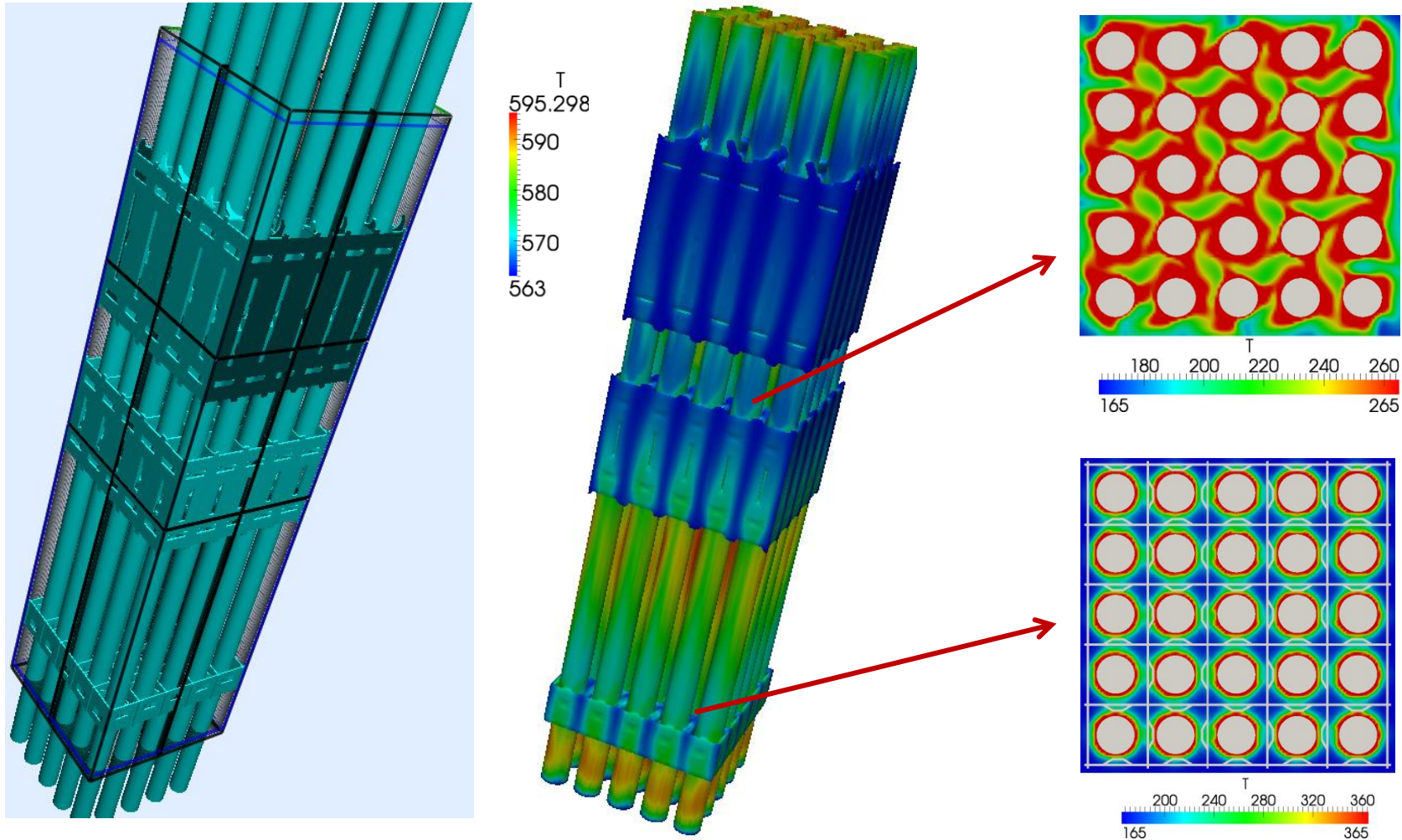
Cross-section interface & temperature



Temperature average results

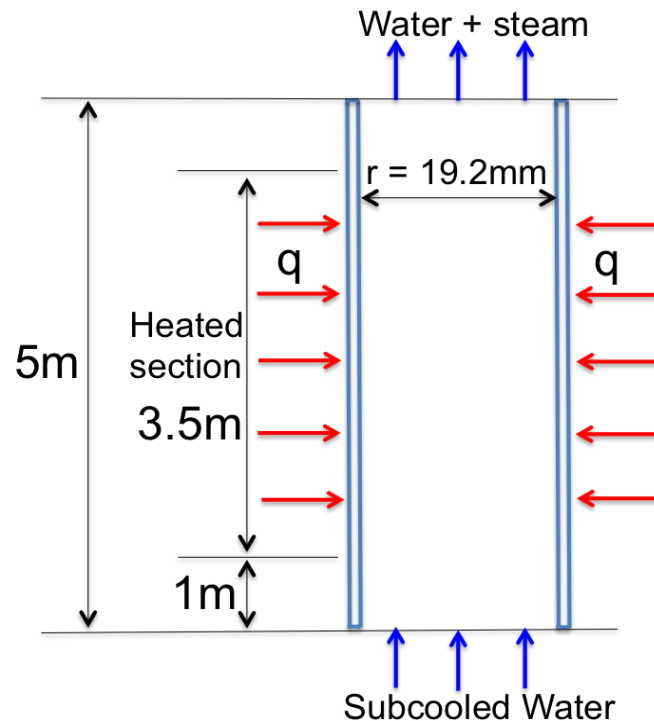


The OECD PSBT 5x5 Benchmark 20



Bubbly-flow boiling: Debora test case (CEA)

DEBORA EXPERIMENTS OF MANON ET AL (2000, 2001)



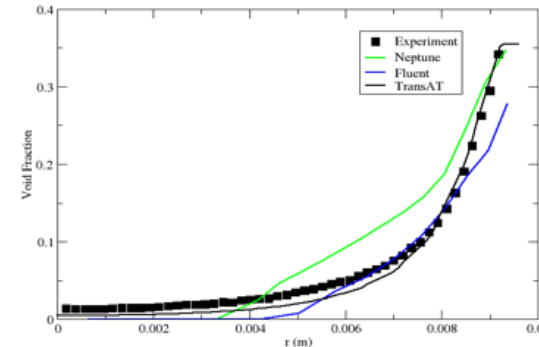
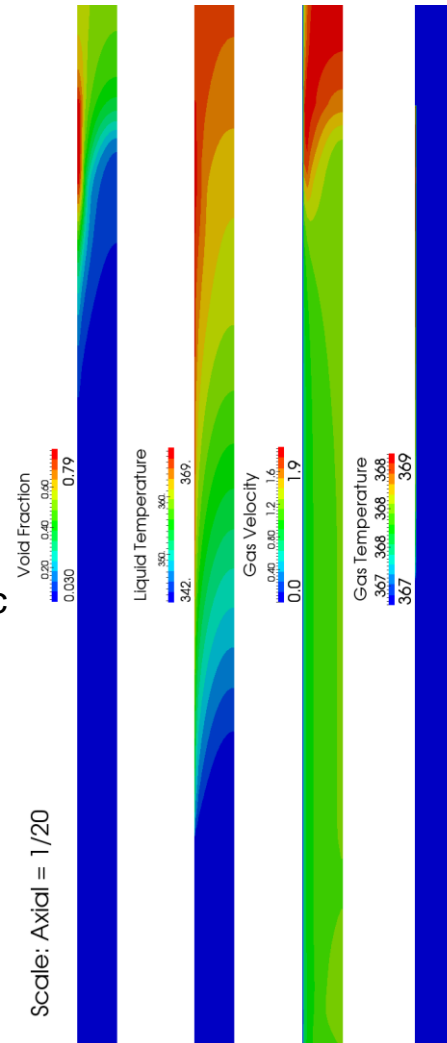
Pipe Length: 5m

Pipe Diameter: 19.2 mm

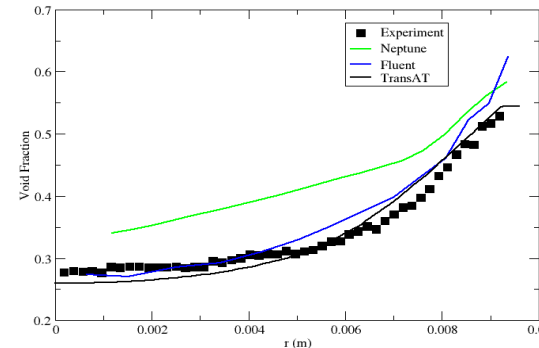
Case	mass flux	T_{inlet}	T_{sat}	Bubble dia
No.	$\text{kg/m}^2/\text{s}$	$^{\circ}\text{C}$	$^{\circ}\text{C}$	mm
1	1006.8	52.97	94.136	0.2
2	1007.4	58.39	94.136	0.58
3	999.5	63.43	94.136	0.65
4	1005	67.89	94.136	3.2
5	1004.8	70.14	94.136	4.0
6	1004.8	72.65	94.136	5.1
7	994.9	73.7	94.136	6.2

Bubbly-flow boiling: Debora test case (CEA)

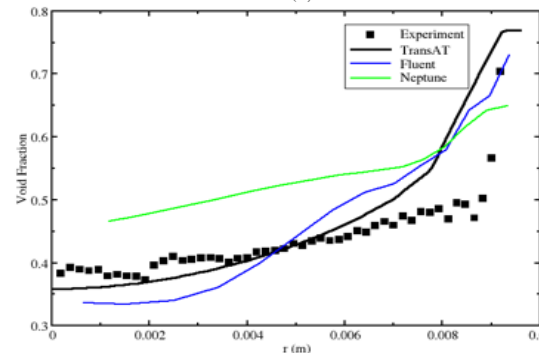
- Iso-contours of transport quantities, including liquid and vapour temperature.
- 2D Axisymmetric simulations TransAT.



Void Fraction for Case 2 & 3:
 $T_{in} = 58.4\text{ C and }63.4\text{ C}$



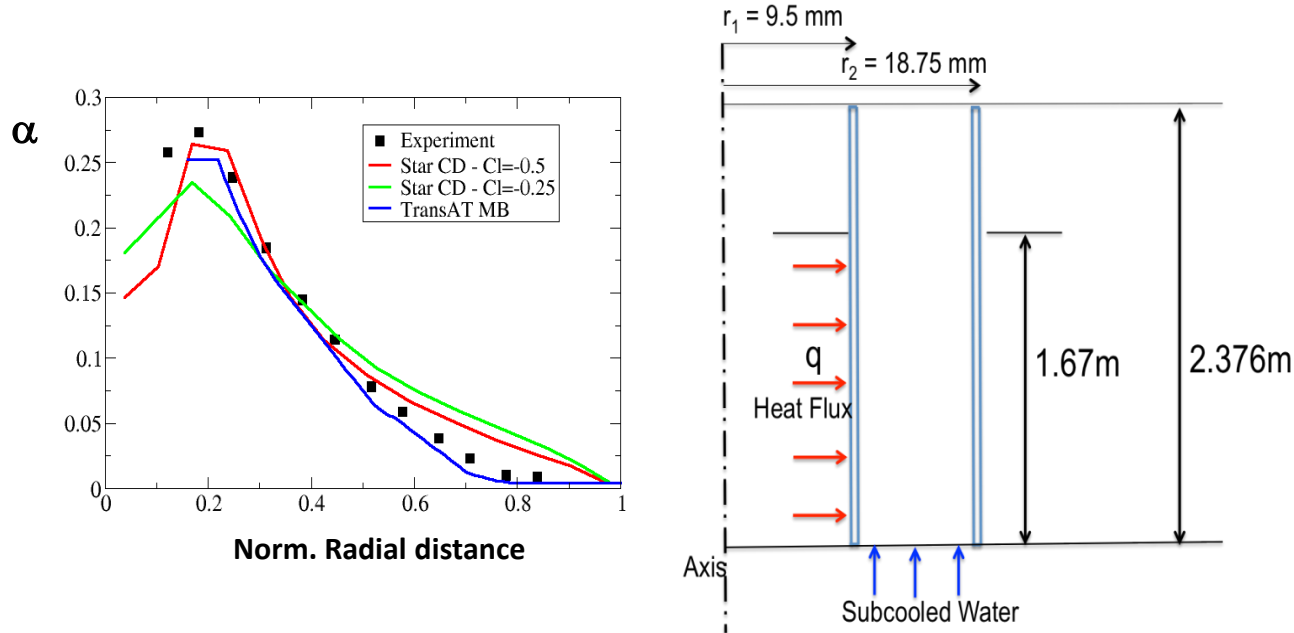
Void Fraction for Case 4 & 5:
 $T_{in} = 67.9\text{ C and }70.14\text{ C}$



Void Fraction for Case 6 & 7:
 $T_{in} = 72.6\text{ C and }73.7\text{ C}$

Bubbly-flow boiling: Lee et al. & Tu & Yeoh (KAERI)

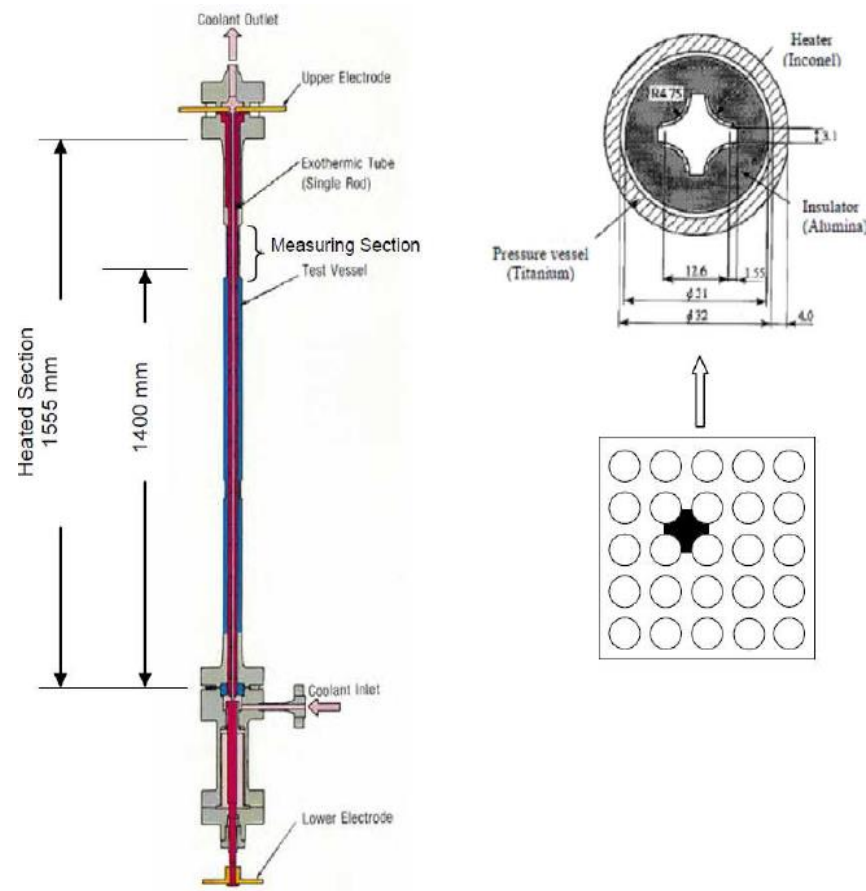
EXPERIMENTS OF LEE, PARK & LEE (2002) AND TU & YEOH (2003)



- Pipe Length: 2.376m
- $q=152.3$ kW/m²
- $G=474$ kg/(m²s)
- $P=0.14$ Mpa
- $\Delta T_{sub}=11.5$ K.

Heat flux	mass flux	T_{inlet}	T_{sat}
MW/ m ²	kg/m ² /s	K	K
0.1523	474	371.5	383

NUPEC PWR Test Facility

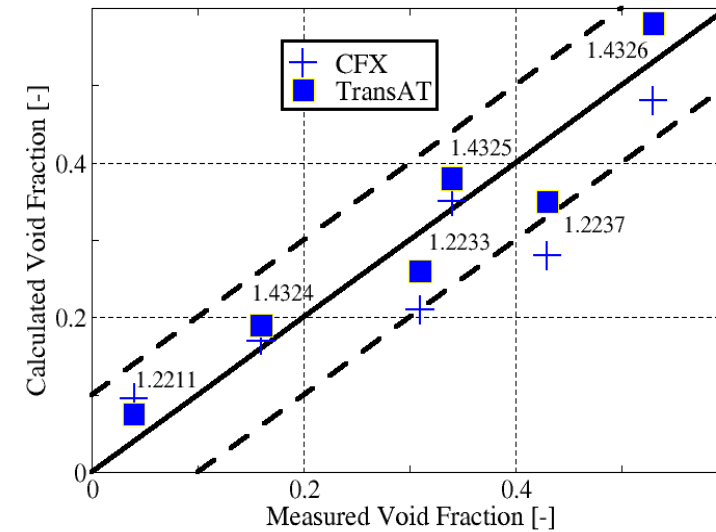
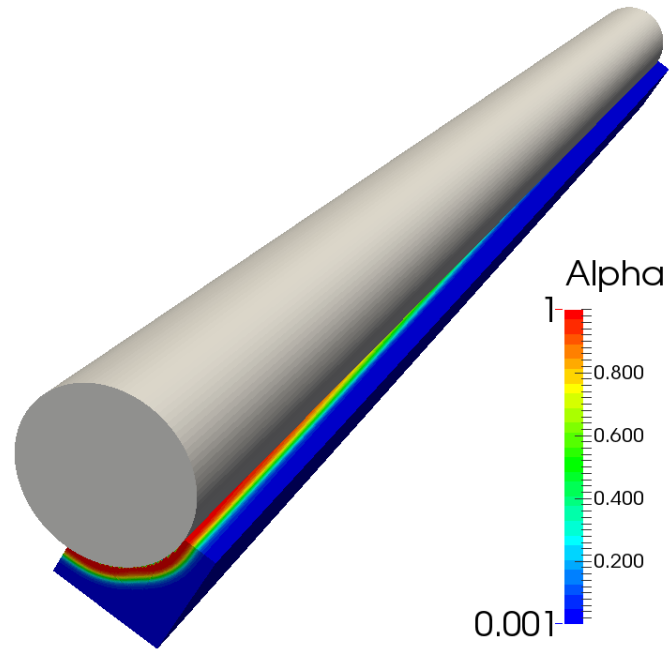


Testcase	Pressure [MPa]	Inlet Temp [°C]	Power [kW]	Mass Flux [kg m ⁻² s ⁻¹]
1.2211	15	295.4	90	11
1.2223	15	319.6	70	11
1.2237	15	329.6	60	11
1.4411	10	238.9	60	5
1.4325	10	253.8	60	2
1.4326	10	268.8	60	5

Cell Size (in mm)	No. of Cells	No. of Processors	Wall Clock Time (in days)
5.31	9216	1	0.33
2.655	73728	8	0.75
1.328	1280000	108	1.5
0.885	2880000	128	4

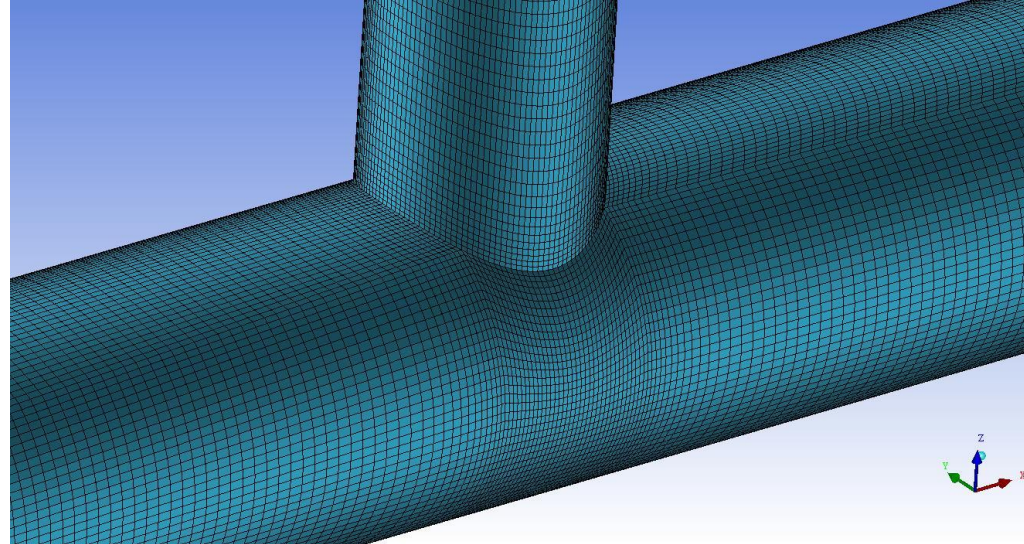
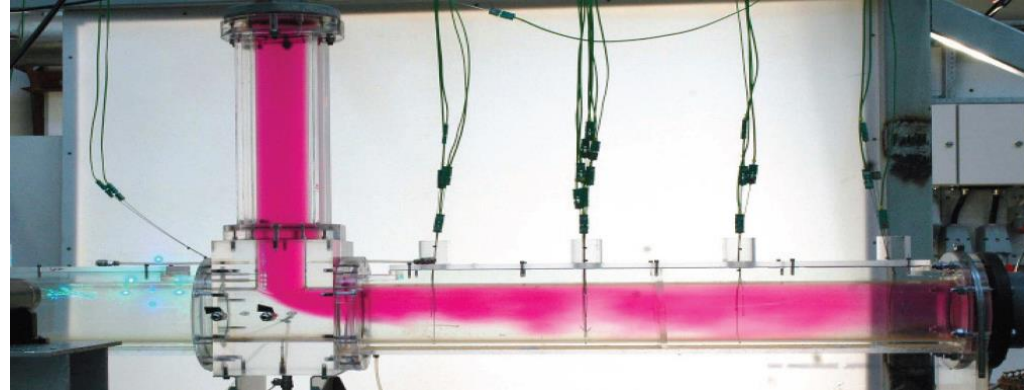
NUPEC PWR Test Facility

- Iso-contours of vapour void fraction.
- Calculated vs. measured space-averaged void fraction.
- Comparison with CFX results

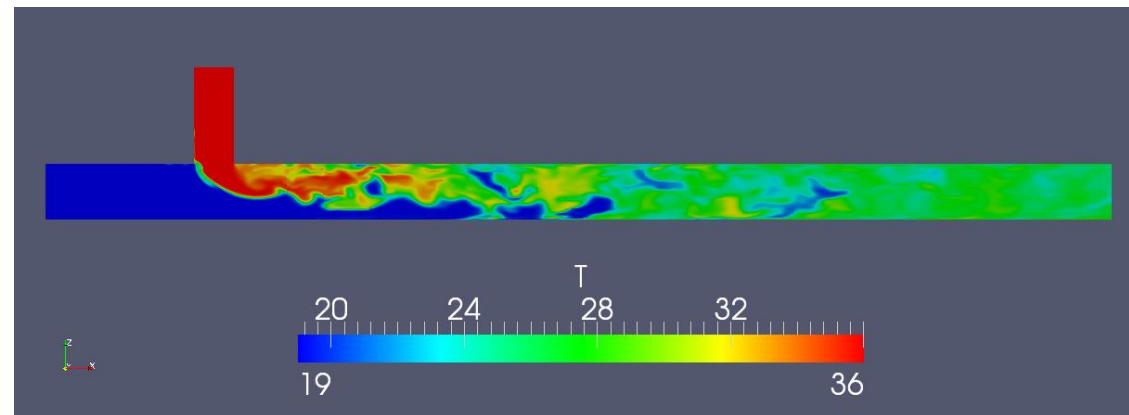
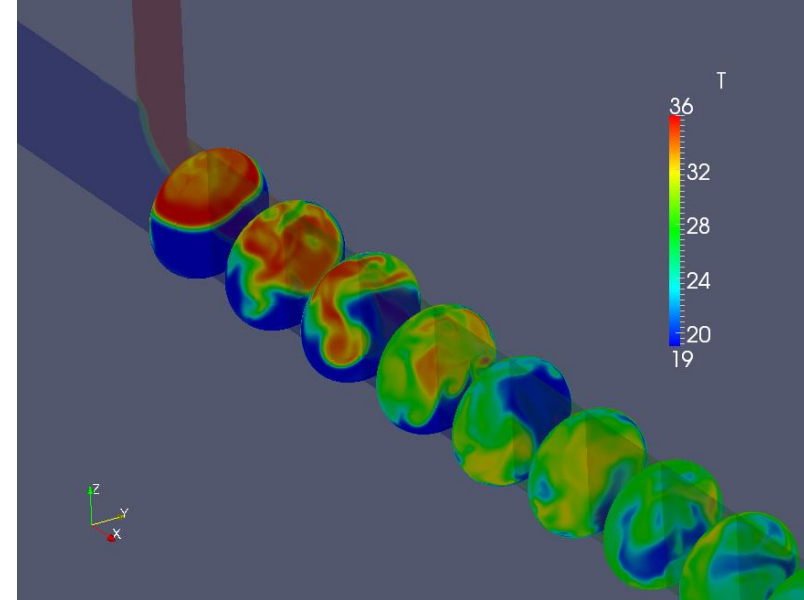
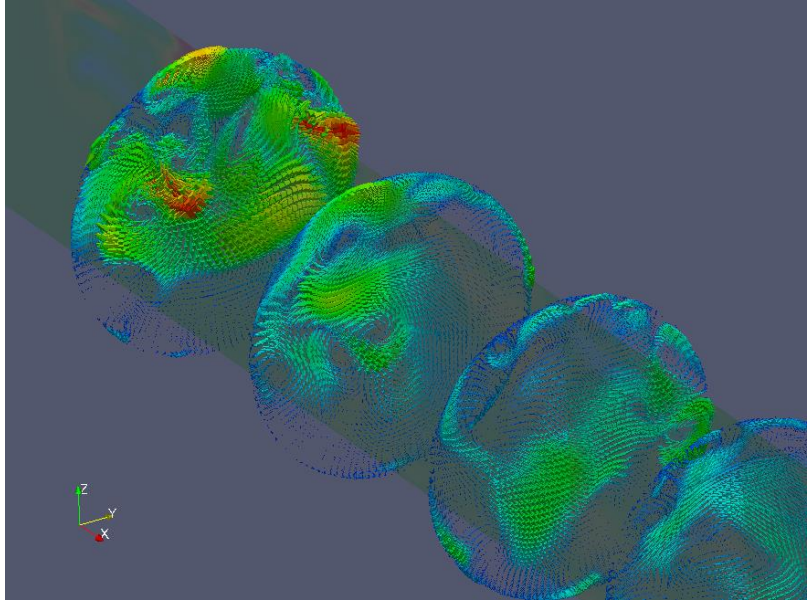


LES of Thermal stripping in a T-junction

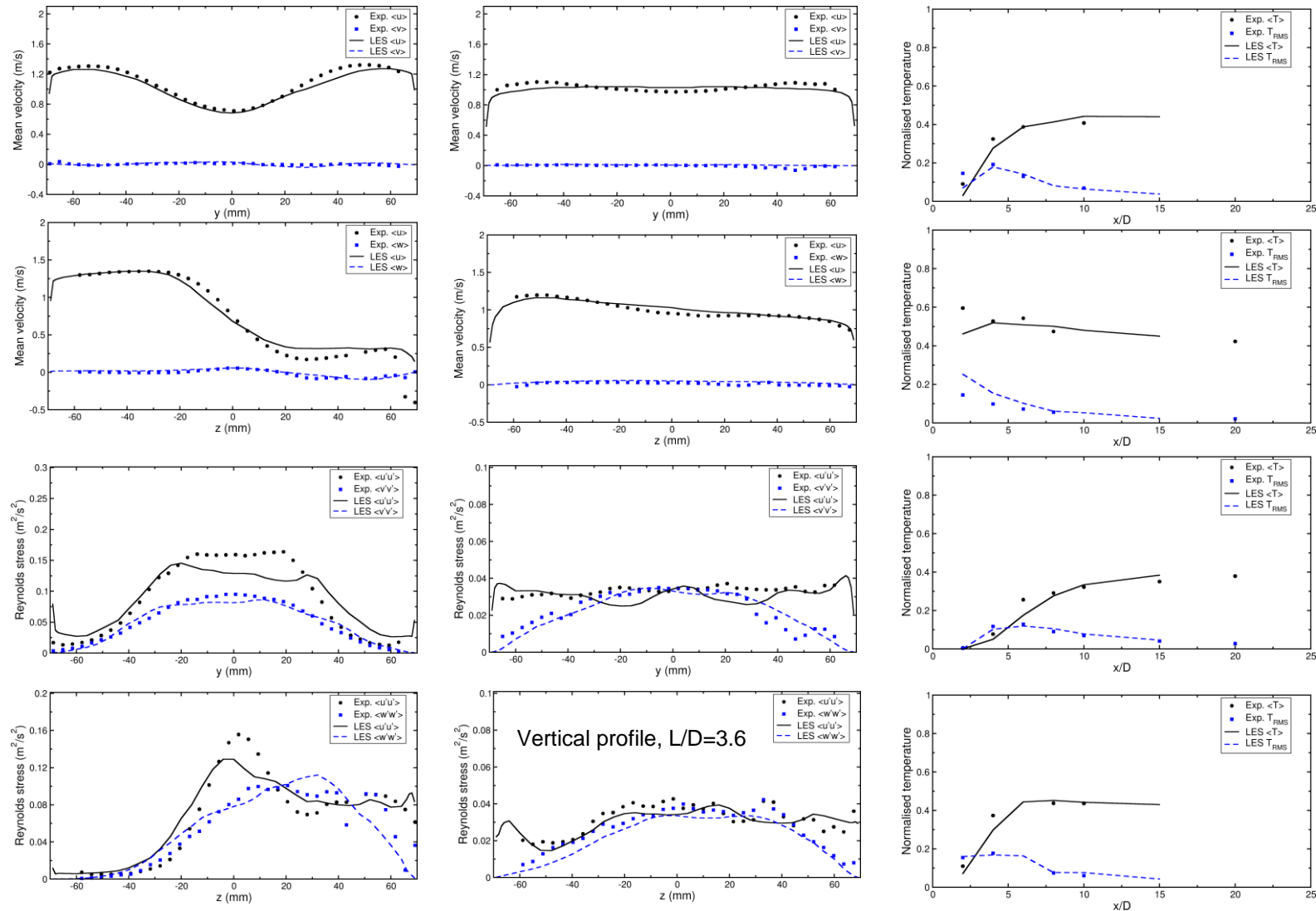
- Flow visualization test in the Vattenfall T-junction test facility (Älvkarleby Labs., Vattenfall R&D).
- $Re = 1.9E5$; $\Delta T = 15$ Deg.
- BFC grid (3 million cells)
- LES with WALE SGS model



Instantaneous results

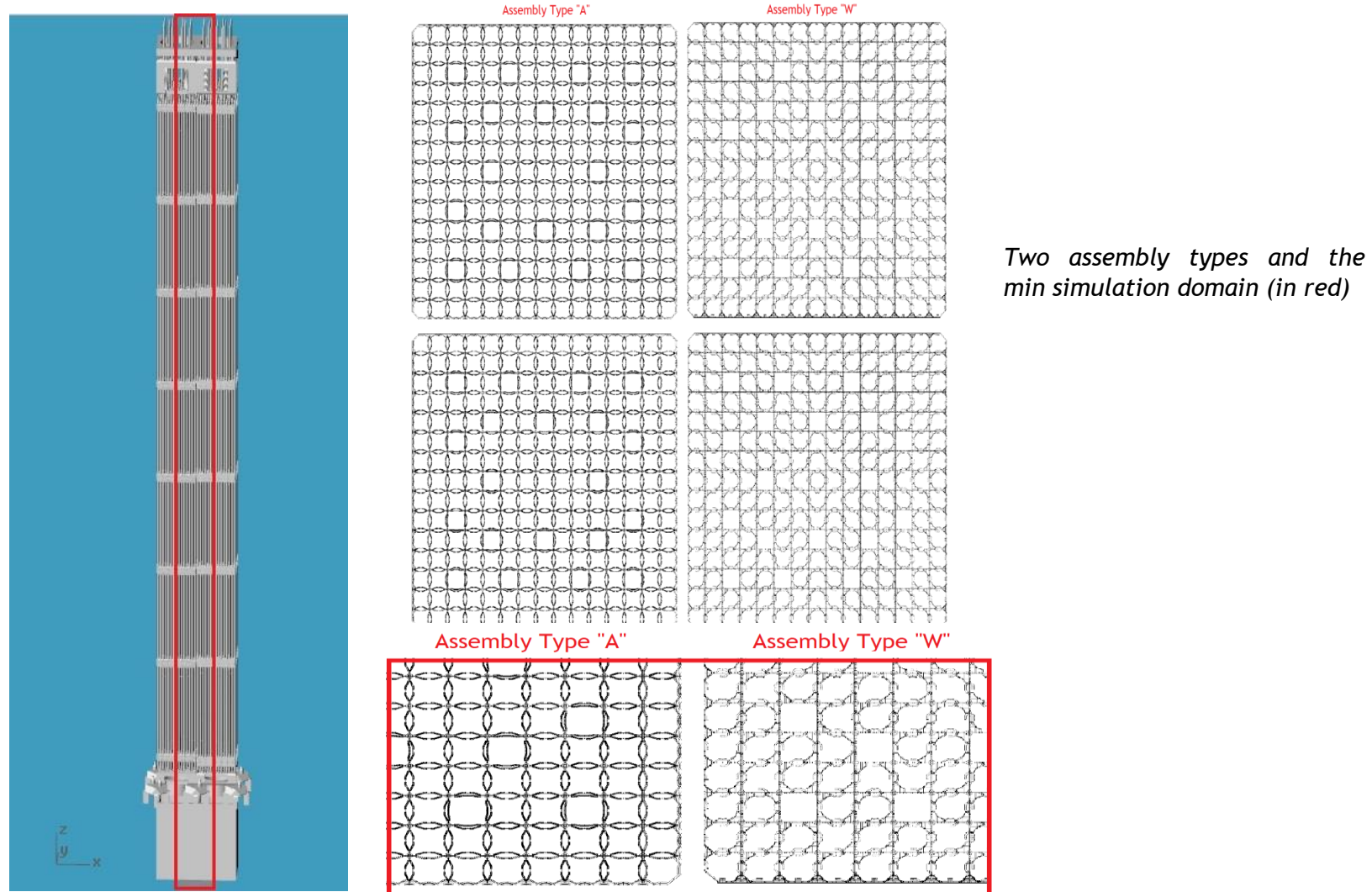


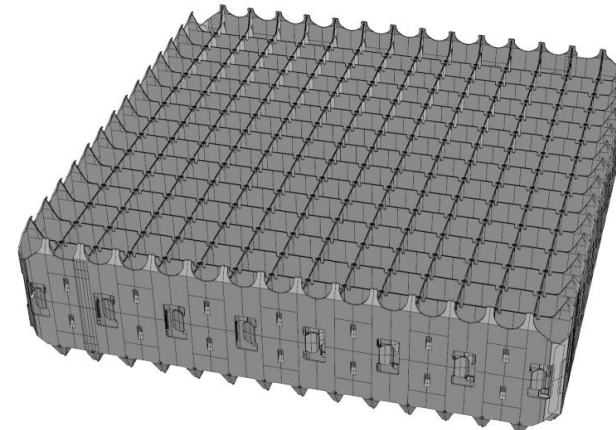
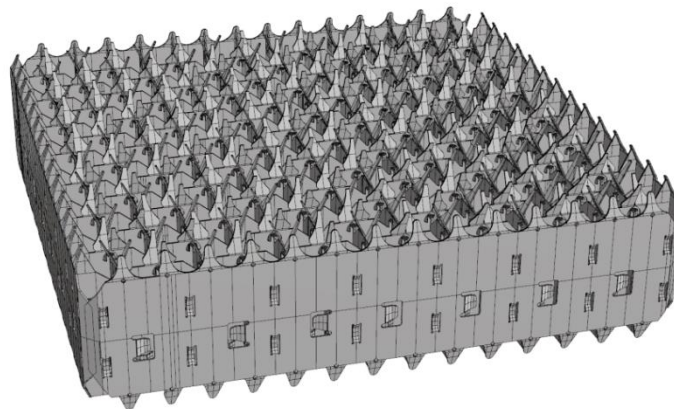
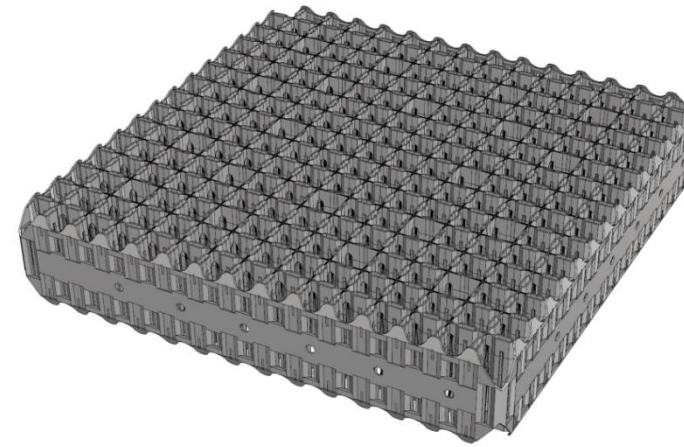
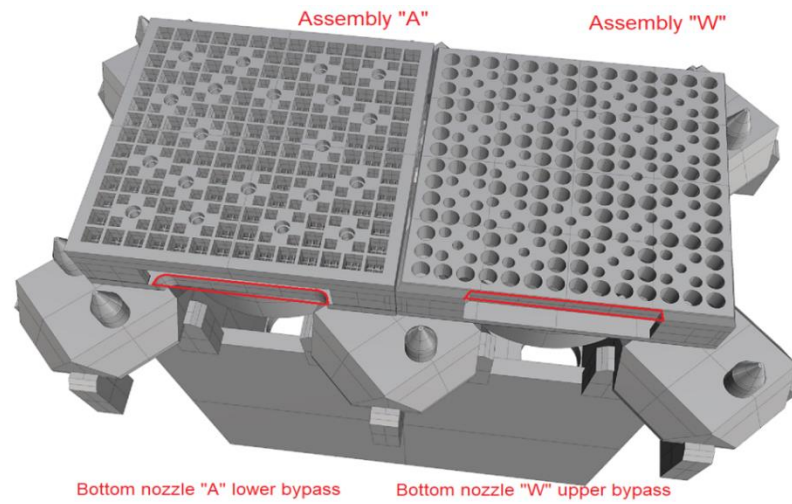
Time average results (mean & r.m.s variables)



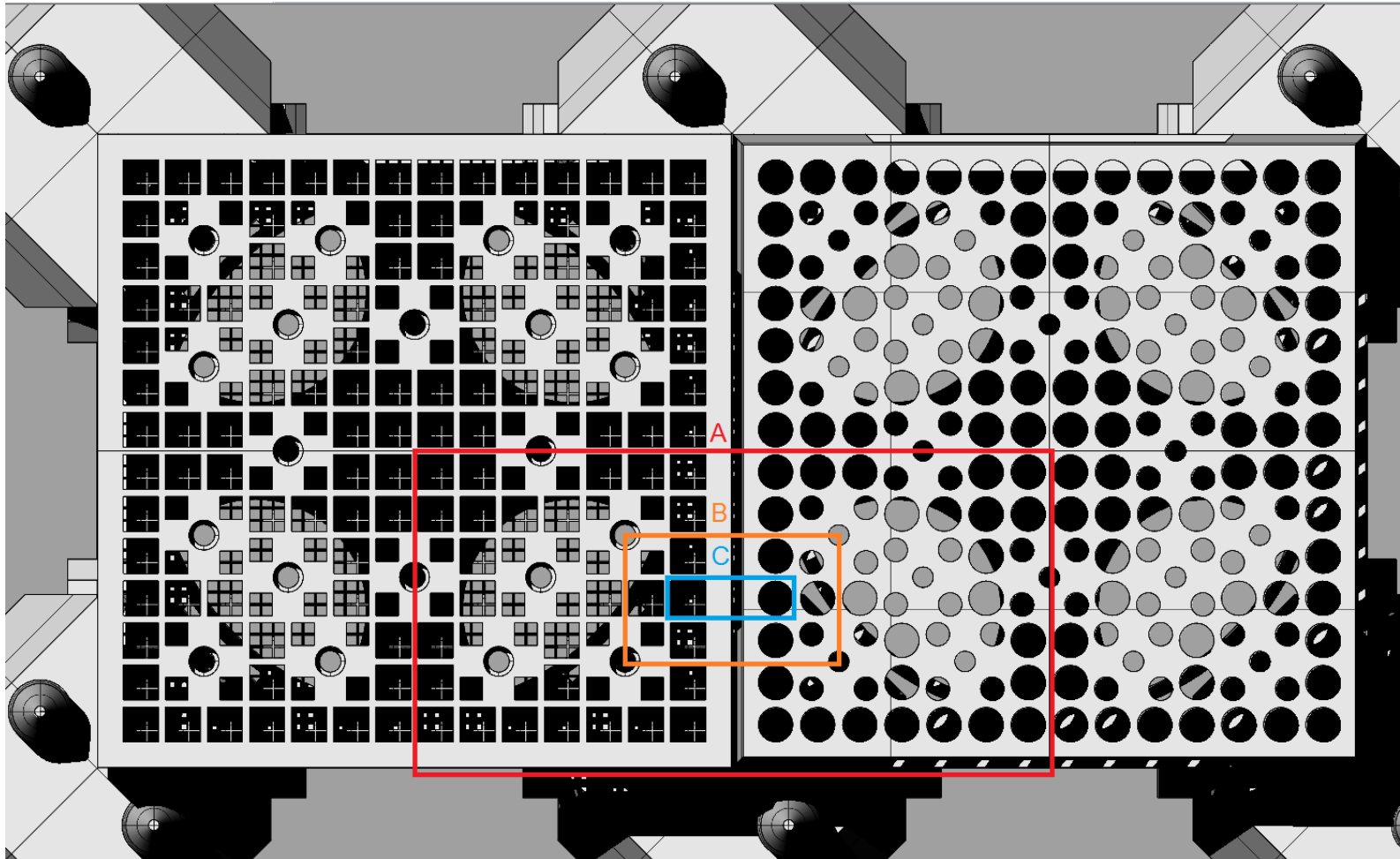
Grand-challenge problem

Convective boiling flow in two types of assemblies





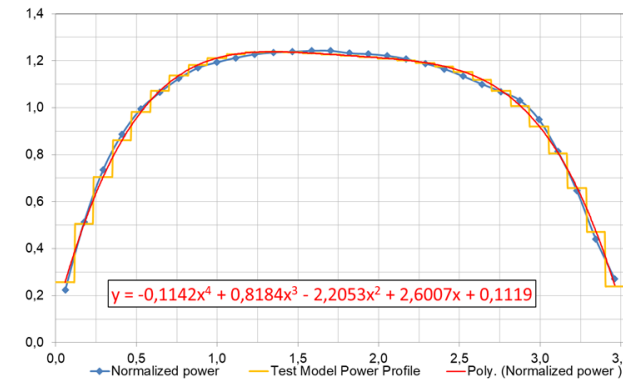
- Bottom nozzle



Parameter	Value
Reactor Power [MWth]	3002
Average Linear Power [W/cm]	235.04
Coolant Inlet Temperature [K]	564.65
Coolant Outlet Average Temperature [K]	599.35
System Pressure [bar]	154
Core mass flow rate [kg/s]	15980
Core volumetric flow rate [m³/s]	21.502
Total core total bypass, mass flow rate [kg/s]	749.46 (=4.69% of core mass flow rate)
Bypass through thimble tubes, m. flow rate [kg/s]	263.67 (=1.65% of core mass flow rate)

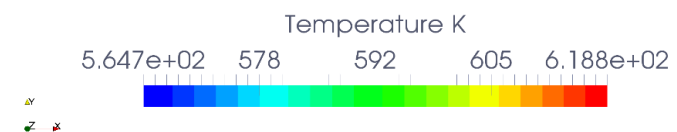
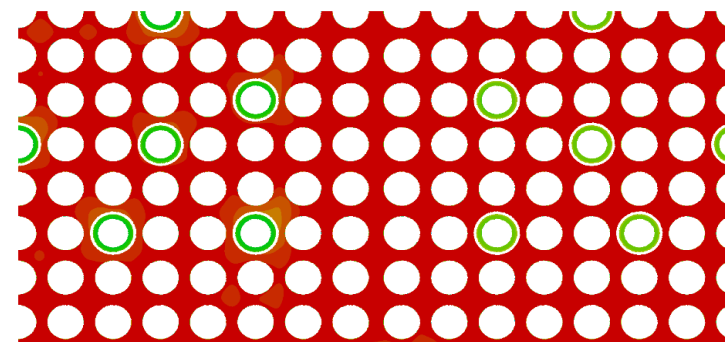
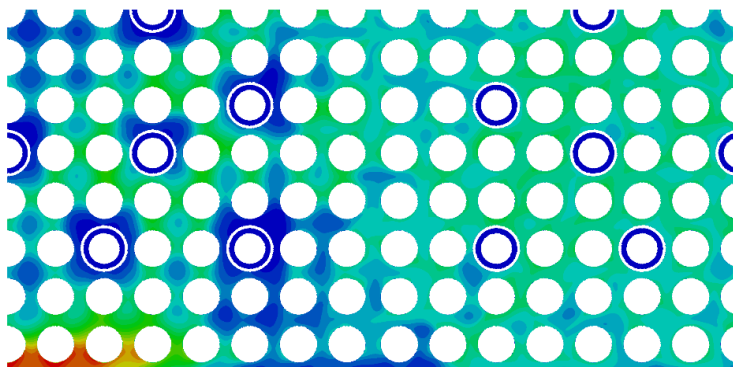
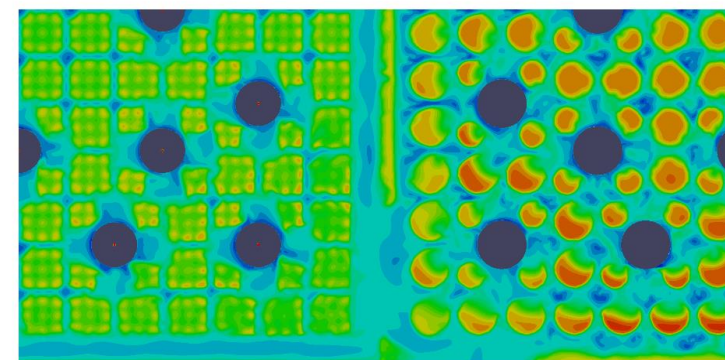
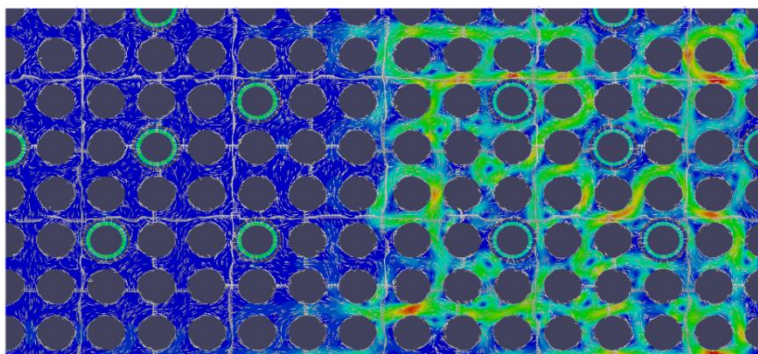
367,1	371,4	395,9	0,0	403,4	382,5	373,6	376,6	H	376,6	373,6	382,5	403,4	0,0	395,9	371,4	367,1
371,4	378,1	389,9	411,5	402,6	406,6	384,3	379,2	G	379,2	384,3	406,6	402,6	411,5	389,9	378,1	371,4
395,9	389,9	396,3	417,5	422,8	0,0	403,6	383,5	F	383,5	403,6	0,0	422,8	417,5	396,3	389,9	395,9
0,0	411,5	417,5	0,0	423,7	414,3	389,5	382,8	E	382,8	389,5	414,3	423,7	0,0	417,5	411,5	0,0
403,4	402,6	422,8	423,7	404,2	408,6	385,5	379,2	D	379,2	385,5	408,6	404,2	423,7	422,8	402,6	403,4
382,5	406,6	0,0	414,3	408,6	0,0	392,6	374,0	C	374,0	392,6	0,0	408,6	414,3	0,0	406,6	382,5
373,6	384,3	403,6	389,5	385,5	392,6	368,1	364,9	B	364,9	368,1	392,6	385,5	389,5	403,6	384,3	373,6
373,6	379,2	383,5	382,8	379,2	374,0	364,9	358,7	A	358,7	364,9	374,0	379,2	382,8	383,5	379,2	373,6
8	7	6	5	4	3	2	1		1	2	3	4	5	6	7	8
Assembly A									Assembly W							

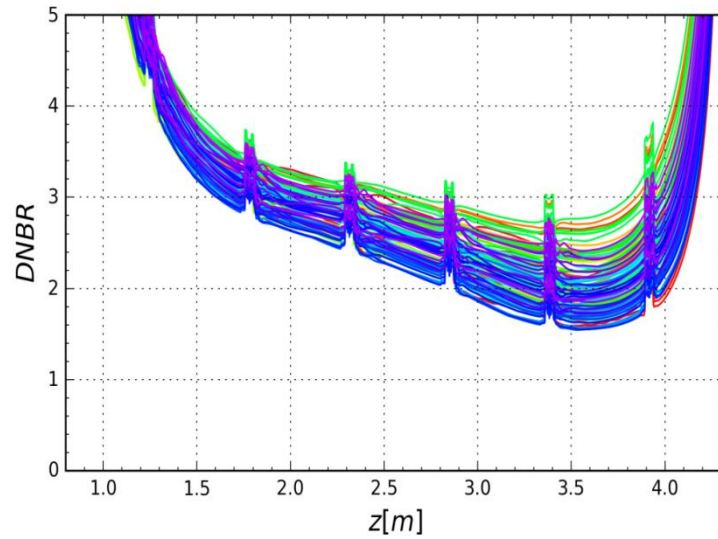
Quarter average assembly power distribution [W/cm] for both assembly



Axial power distribution and fitted shape function

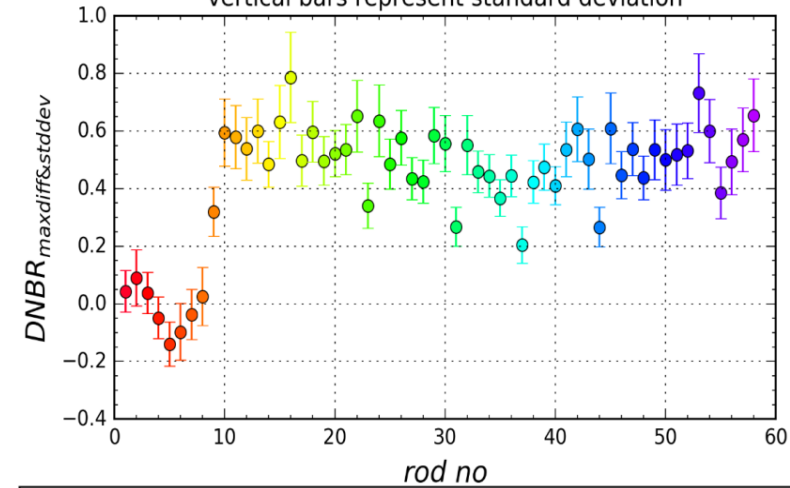
#	Region	Axial Coordinate [mm]			Sub. Seg. [mm]	$\Delta x = \Delta y$ [mm]	AR	Segment # Δx_{seg} [mm] Cells
		Z_{start}	Z_{end}	ΔZ				
1	Domain extention and Bott. plate	-50	385	385	435	0.25	10	1
2	Bottom nozzle lower part	385	554	604	169	0.25	10	
3	Bottom nozzle filter and bottom spacers	554	742	792	188	0.25	1	
4	Rods	742	1120	1170	378	0.25	10	1170 4.362E+08
5	Guide tube hole	1120	1212	1262	92	0.25	1	2
6	2 nd spacers	1212	1306	1356	94	0.25	1	
7	Rods	1306	1673	1723	367	0.25	10	553 3.366E+08
8	Rods	1673	1746	1796	73	0.25	10	3
9	3 rd Spacers and sleeves	1746	1839	1889	93	0.25	1	
10	Rods	1839	2207	2257	368	0.25	10	534 2.142E+08
11	Rods	2207	2280	2330	73	0.25	10	4
12	4 th Spacers and sleeves	2280	2373	2423	93	0.25	1	
13	Rods	2373	2740	2790	367	0.25	10	533 2.144E+08
14	Rods	2740	2813	2863	73	0.25	10	5
15	5 th Spacers and sleeves	2813	2907	2957	94	0.25	1	
16	Rods	2907	3275	3325	368	0.25	10	535 2.147E+08
17	Rods	3275	3346	3396	71	0.25	10	6
18	6 th Spacers and sleeves	3346	3441	3491	95	0.25	1	
19	Rods	3441	3808	3858	367	0.25	10	533 2.144E+08
20	Rods	3808	3879	3929	71	0.25	10	7
21	7 th Spacers and sleeves	3879	3972	4022	93	0.25	1	
22	Rods	3972	4335	4385	363	0.25	10	527 2.136E+08
24	Rods	4335	4403	4453	68	0.25	10	8
25	8 th Spacers and sleeves	4403	4512	4562	109	0.25	1	
26	Region above rods up to guide tubes end plug	4512	4570	4620	58	0.25	1	665
27	Top nozzle and upper plate	4570	4753	4803	183	0.25	10	3.329E+08
28	Upper plate and domain extention	4753	5000	5000	247	0.25	10	
Total					5050	-	-	2.177E+09
Total fine meshing					859	0.25	1	1.278E+09
Total coarser meshing					4191	0.25	10	8.993E+08



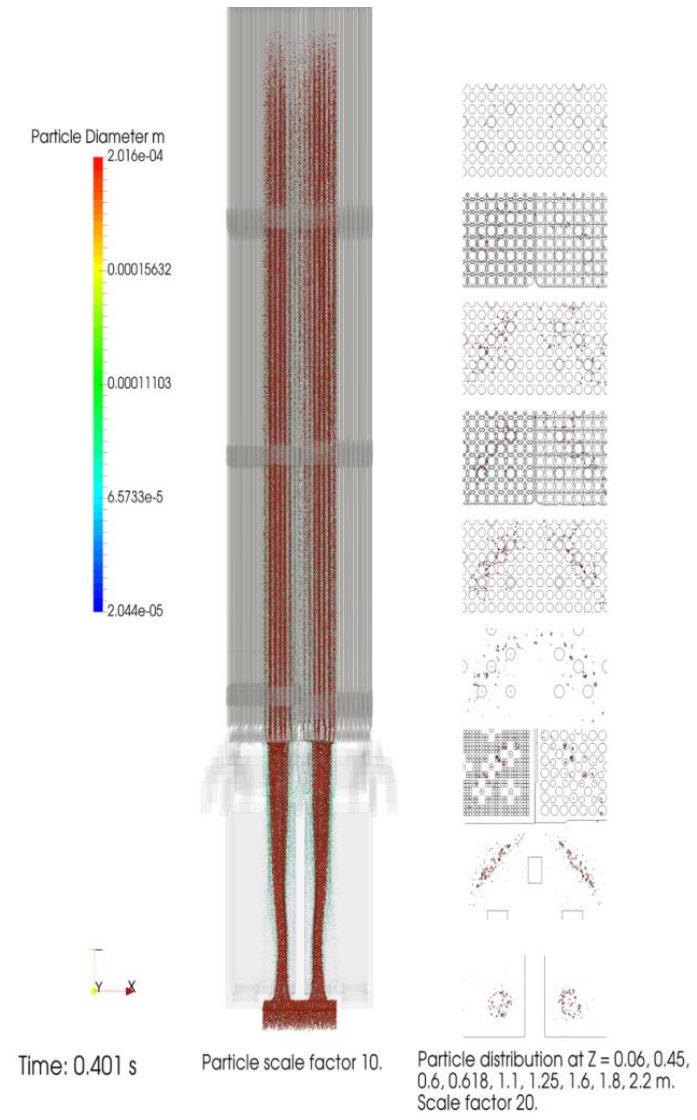
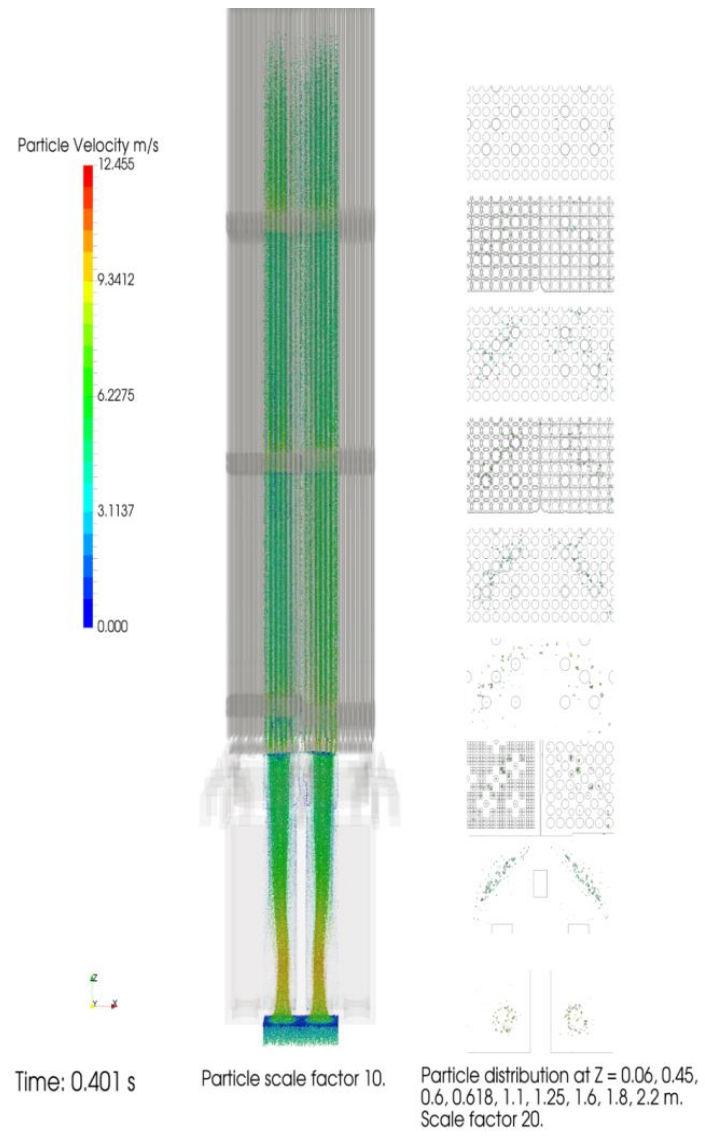


_rod_A_A1	_rod_A_D3	_rod_A_G5	_rod_B_B5	_rod_B_E7
_rod_A_A2	_rod_A_D4	_rod_A_G6	_rod_B_B6	_rod_B_F1
_rod_A_A3	_rod_A_D5	_rod_A_G7	_rod_B_B7	_rod_B_F2
_rod_A_A4	_rod_A_D6	_rod_A_G8	_rod_B_B8	_rod_B_F4
_rod_A_A5	_rod_A_D7	_rod_A_H1	_rod_B_C1	_rod_B_F5
_rod_A_A6	_rod_A_D8	_rod_A_H2	_rod_B_C2	_rod_B_F6
_rod_A_A7	_rod_A_E1	_rod_A_H3	_rod_B_C4	_rod_B_F7
_rod_A_A8	_rod_A_E2	_rod_A_H4	_rod_B_C5	_rod_B_F8
_rod_A_B1	_rod_A_E3	_rod_A_H6	_rod_B_C7	_rod_B_G1
_rod_A_B2	_rod_A_E4	_rod_A_H7	_rod_B_C8	_rod_B_G2
_rod_A_B3	_rod_A_E6	_rod_A_H8	_rod_B_D1	_rod_B_G3
_rod_A_B4	_rod_A_E7	_rod_B_A1	_rod_B_D2	_rod_B_G4
_rod_A_B5	_rod_A_F1	_rod_B_A2	_rod_B_D3	_rod_B_G5
_rod_A_B6	_rod_A_F2	_rod_B_A3	_rod_B_D4	_rod_B_G6
_rod_A_B7	_rod_A_F4	_rod_B_A4	_rod_B_D5	_rod_B_G7
_rod_A_B8	_rod_A_F5	_rod_B_A5	_rod_B_D6	_rod_B_G8
_rod_A_C1	_rod_A_F6	_rod_B_A6	_rod_B_D7	_rod_B_H1
_rod_A_C2	_rod_A_F7	_rod_B_A7	_rod_B_D8	_rod_B_H2
_rod_A_C4	_rod_A_F8	_rod_B_A8	_rod_B_E1	_rod_B_H3
_rod_A_C5	_rod_A_G1	_rod_B_B1	_rod_B_E2	_rod_B_H4
_rod_A_C7	_rod_A_G2	_rod_B_B2	_rod_B_E3	_rod_B_H6
_rod_A_C8	_rod_A_G3	_rod_B_B3	_rod_B_E4	_rod_B_H7
_rod_A_D1	_rod_A_G4	_rod_B_B4	_rod_B_E6	_rod_B_H8
_rod_A_D2				

Max difference in DNBR between assembly A and W
in the range of 50-90% of active length,
vertical bars represent standard deviation



1_rod_A_A1_rod_B_A1	16_rod_A_B8_rod_B_B8	31_rod_A_E1_rod_B_E1	45_rod_A_G2_rod_B_G2
2_rod_A_A2_rod_B_A2	17_rod_A_C1_rod_B_C1	32_rod_A_E2_rod_B_E2	46_rod_A_G3_rod_B_G3
3_rod_A_A3_rod_B_A3	18_rod_A_C2_rod_B_C2	33_rod_A_E3_rod_B_E3	47_rod_A_G4_rod_B_G4
4_rod_A_A4_rod_B_A4	19_rod_A_C4_rod_B_C4	34_rod_A_E4_rod_B_E4	48_rod_A_G5_rod_B_G5
5_rod_A_A5_rod_B_A5	20_rod_A_C5_rod_B_C5	35_rod_A_E6_rod_B_E6	49_rod_A_G6_rod_B_G6
6_rod_A_A6_rod_B_A6	21_rod_A_C7_rod_B_C7	36_rod_A_E7_rod_B_E7	50_rod_A_G7_rod_B_G7
7_rod_A_A7_rod_B_A7	22_rod_A_C8_rod_B_C8	37_rod_A_F1_rod_B_F1	51_rod_A_G8_rod_B_G8
8_rod_A_A8_rod_B_A8	23_rod_A_D1_rod_B_D1	38_rod_A_F2_rod_B_F2	52_rod_A_H1_rod_B_H1
9_rod_A_B1_rod_B_B1	24_rod_A_D2_rod_B_D2	39_rod_A_F4_rod_B_F4	53_rod_A_H2_rod_B_H2
10_rod_A_B2_rod_B_B2	25_rod_A_D3_rod_B_D3	40_rod_A_F5_rod_B_F5	54_rod_A_H3_rod_B_H3
11_rod_A_B3_rod_B_B3	26_rod_A_D4_rod_B_D4	41_rod_A_F6_rod_B_F6	55_rod_A_H4_rod_B_H4
12_rod_A_B4_rod_B_B4	27_rod_A_D5_rod_B_D5	42_rod_A_F7_rod_B_F7	56_rod_A_H6_rod_B_H6
13_rod_A_B5_rod_B_B5	28_rod_A_D6_rod_B_D6	43_rod_A_F8_rod_B_F8	57_rod_A_H7_rod_B_H7
14_rod_A_B6_rod_B_B6	29_rod_A_D7_rod_B_D7	44_rod_A_G1_rod_B_G1	58_rod_A_H8_rod_B_H8
15_rod_A_B7_rod_B_B7	30_rod_A_D8_rod_B_D8		





Making Future

- Advanced Modelling & Simulation
- www.afry.com/ams; ams@afry.com